Characterization of interleukin-4 induced gene-1 (IL-4I1) as a host immunoregulator to cutaneous leishmaniasis in cell-based models

Aya Fouad

Thesis presented for the degree of Master of Science in the Department of Molecular and Cell Biology, Faculty of Science, University of Cape Town

Supervisor: Dr Ramona Hurdayal

February 2022

Plagiarism Declaration

‘I Aya Fouad know the meaning of plagiarism and declare that all of the work in the dissertation (or thesis), save for the properly acknowledged, is my own’.

Signature: Signed by candidate

Acknowledgments

It takes a village to accomplish your goals, and I would like to take this time to thank all those that supported, motivated, and guided me throughout this journey.

Firstly, to my supervisor, Dr Ramona Hurdayal. I am in constant awe of your accomplishments, and I could not have finished this journey without your constant guidance. Thank you for allowing me the space to make mistakes and to learn. Thank you for trusting me to do my best and thank you for pushing me to the limits of what I thought I could accomplish. I will forever be grateful to have had a mentor, tutor, and supervisor such as yourself. I wish you nothing but happiness and peace as you start your new journey.

I would like to thank past and present members of the *Leishmania* research group. To Zama Cele, Raphael Aruleba, Bradley Wonderlik, Priscilla Opare, Rebeng Maine, Fran Prenan, Nikhil Amtha, and Bernard Osero, thank you for the help, reagents, memories and laughs we shared in the lab.

To all those at the Research Animal Facility (RAF), especially Dr Rodney Lucas for training me to handle the mice. Those at the Molecular and Cell Biology (MCB) especially Ms Maureen Adams for her humour and assistance. To Mrs Shakiera Sattar for training me in the Biosafety Level II facility, thank you. To Mr Rudranil Hazra for his guidance in working with siRNAs, thank you. To Mr Nicholas Crowther for editing and checking my thesis, thank you. To the staff and baristas at various Seattle Coffee Co and Vida e Caffe shops, your smiles and warm welcomes until closing time will forever hold a special place in my heart, thank you.

I would like to offer my deepest gratitude to my beloved friends. To Sophia Bam, Rachel Hunter, Mariam El Sherbini, I have no words to describe how each of you shaped and guided my journey as a MSc Candidate. This is as much your accomplishment as it is mine. Thank you.

This journey would not have been the same without the constant guidance and support from Mr Youssef El Dash. Thank you for pushing me at times when I wanted to walk away.

Finally, to my rocks. My brother and my Mama. The past 3 years have been an adventure that would have been boring and dull without you. Thank you for hearing me complain and for allowing me to annoy you with my research. I cannot thank you enough for the constant supply of help, motivation, guidance, love, time, and petrol that you both have offered. Thank you for you.

I dedicate this thesis to my late father, who I know has been by my side throughout this journey. I am who I am because of you.

Funding: This research was supported by the Thuthuka Fund from the National Research Foundation (NRF), South Africa and from the Post Graduate Funding Office (PGFO), University of Cape Town, South Africa.

Table of Contents

List of Figures

List of Tables

Abstract

Macrophage activation can be split into two distinct groups: Classically-Activated (M1) and Alternatively-Activated (M2) macrophages. Each are associated with a certain immune response; in the context of cutaneous leishmaniasis caused by infection with *Leishmania major*. Specifically, M1 macrophages allow for disease control through stimulation of cytokines such as IFN-γ and release of nitric oxide for killing of intracellular parasites. Contrastingly, M2 macrophages allow for parasite survival through stimulation of cytokines such as IL-4 and IL-13 and release of urea that supports parasite growth. Candidate genes responsible for promoting M1 or M2 macrophages are being investigated as the macrophage is the sight of infection for leishmaniasis. One such candidate is *IL-4i1*, which has been shown to be responsible for M2 polarization. Notably, IL-4i1 catalyses phenylalanine, water, and oxygen to produce phenylpyruvate, ammonia and hydrogen peroxide. Interestingly, high levels of hydrogen peroxide create a toxic cellular environment and has been shown to lead to parasite destruction. Due to these contrasting roles of IL-4i1, IL-4i1 may be pivotal in modulating macrophage activation and host response to infection. Accordingly, we investigated *IL-4i1* in a murine and human cutaneous leishmaniasis (CL) cell-based model using bone marrow-derived macrophages (BMDMs) derived from BALB/c IL-4i1$^{+/+}$ and IL-4i1$^{-/-}$ mice and silencing of *IL-4i1* in THP-1-derived macrophages. THP-1 monocytes were differentiated into macrophages via phorbol 12-myristate 13-acetate (PMA). Following macrophage verification, THP-1-derived macrophages were silenced with IL-4i1 siRNA constructs using the Silencer SelectTM siRNA Construction kit and Lipofectamine 3000 transfection agent. In IL-4 and IFN-γ-stimulated IL-4i1$^{-/-}$ BMDM infected with *L. major,* an increase in parasite burden was found ($p<0.05$, 24 hr PI). Immunologically, nitrite was reduced, and levels of IL-12 were below detection limit whilst IL-10 was increased upon IL-4 stimulation, compared to IL-4i1$^{+/+}$. Thus, the presence of IL-4i1 may play a role in controlling parasite replication and mediating M1 polarization. After 24h of infection with *L. major*, *IL-4i1*-silenced THP-1-derived macrophages showed increases in production of nitrite ($p<0.005$) and a decrease in parasite burden ($p<0.05$), hence the absence of *IL-4i1* induced M1 activation. Collectively, these data indicate that IL-4i may indeed favour M2 activation in the context of *L. major* infection as absence thereof promoted a detrimental environment

for parasite burden. Altogether, this underscores IL-4i1 as a potential susceptibility factor to CL. Understanding how *Leishmania* parasites can modify host immune response could lead to identifying novel therapeutics such as host-directed therapies.

1. Introduction

1.1 Neglected tropical disease (NTDs) and response towards combating them

A neglected tropical disease (NTD) is a group of emerging infectious diseases (EID). NTDs are diseases that occur in tropical and sub-tropical climates and have been linked to poverty (Engels and Zhou, 2020). EIDs are defined as disease that have been either newly discovered, recognised, introduced, or evolved (Petersen *et al*., 2018). These diseases have a high rate of mutation and usually expand geographically due to climate change, human demographics, and travel. This could also be achieved if they extend their range of hosts and vectors, which could also occur due to microbial adaptation, changing ecosystems and human susceptibility to infection (Fenollar 2018; Zellweger *et al*., 2017).

A range of factors affecting NTDs have been reported (Fenollar and Mediannikov, 2018, Morens *et al*., 2004, Jones *et al*., 2008, Petersen *et al*., 2018). The two main factors of NTDs include socioeconomic status (poverty) and the persistence of zoonotic infections (Engels and Zhou, 2020; Jones *et al*., 2008; Zellweger *et al*., 2017).

To tackle this issue, world leaders have agreed to work together to identify new ways in which vaccines and possible treatments can be explored for NTDs such as leishmaniasis (Røttingen *et al*., 2017). An organization called the Emerging Infections Task Force aims to create a network of established experts in infectious diseases to raise awareness about NTDs such as leishmaniasis in endemic areas. Another is the Coalition for Epidemic Preparedness Innovation (CEPI) compromising 200 experts and 80 organizations. A prime example of an NTD that is also an EID is leishmaniasis.

1.2 Leishmaniasis

This disease is classed as a zoonotic infection thereby giving emphasis to its NTD and EID nature as discussed above. Parasites are transmitted to mammalian hosts by the bite of an infected female sandfly of the genus *Phlebotominae*. Leishmaniasis was first discovered in the Middle Ages and has since spread to very continent except Antarctica, particularly prevalent in tropical and subtropical regions of the world (Palma *et al*., 2021; Steverding, 2017).

1.2.1 Lifecycle

Leishmaniasis is transmitted through the bloodmeal of the sandfly from the *Phlebotomus* genus (Choi and Lerner, 2001). Parasites have a dimorphic lifecycle. The first half of the cycle is within the gut of the female sandfly as elongated, motile, and flagellated promastigotes, (**Figure 1.1**), while the second half is spent in the phagolysosome of mammalian macrophages as round and non-motile amastigotes (Inbar *et al*., 2017; Mojtahedi *et al*., 2008).

The gut microbiome of the sandfly has been reported to influence the growth conditions of the parasite (Inbar *et al*., 2017; Mukhopadhyay *et al*., 2012). Since it is the start of the parasite lifecycle and when the sandfly takes a bloodmeal, it will inject motile, elongated promastigotes into the skin (Govender *et al*., 2018). When they are phagocytosed by macrophages, the promastigotes will differentiate into non-motile, round amastigotes amastigotes without flagella. As shown in **Figure 1.1,** amastigotes will multiple and eventually burst open the macrophage, making the amastigotes free to infect other cells. If another sandfly takes a bloodmeal from an infected person, the amastigotes will develop flagella and convert to their promastigote form, whereupon the cycle repeats (Hurdayal *et al*., 2017).

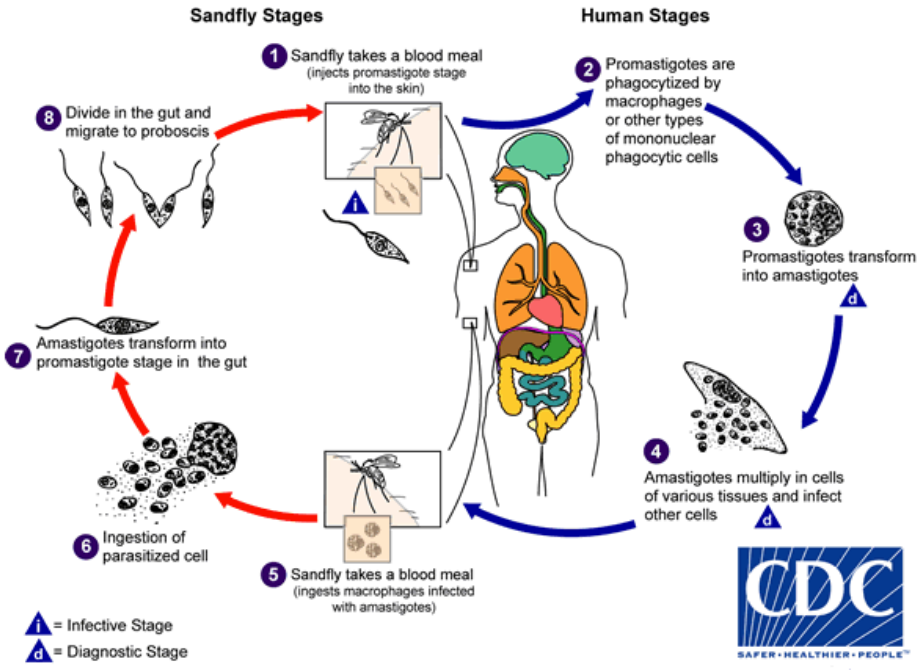

Figure 1.1: Dimorphic lifecycle of *Leishmania* parasite in gut of *Phlebotomine* sandfly and mammalian host. The sandfly injects promastigotes during a bloodmeal where the promastigotes are phagocytosed by macrophages. Within the macrophage, promastigotes will differentiate into amastigotes without flagella. Subsequently, amastigotes will multiple and eventually rupture the macrophage where the amastigotes are now released to the cell microenvironment. Now, they may infect neighbouring macrophages and if another sandfly takes a bloodmeal from an infected person, the amastigotes will develop flagella and convert to their promastigote form. Within the sandfly gut, the cycle will start again (CDC, 2020).

1.2.2 Epidemiology and clinical spectrum

Leishmaniasis is endemic in 102 countries with 350 million diagnoses globally (Kaye and Scott, 2011; Osero *et al*., 2020). A more recent study shows that there are 0.7 to 1 million new cases every year from an estimated about 100 endemic countries (Burza *et al*., 2018). One of the major factors affecting the spread of leishmaniasis is the socioeconomic and environmental determinants in certain parts of the world (Guzman and Istúriz, 2010). These areas specifically have been linked to vegetation coverage, rainfall, humidity, and temperature (Messina *et al*.,

2015; Zellweger *et al*., 2017; Descloux *et al*., 2012; Hii *et al*., 2012). However, higher incidence rates of infection were found within lower socioeconomic statuses i.e., areas where unemployment rates were high. Other socioeconomics factors include revenue and housing quality (Reiter *et al*., 2003; de Mattos Almeida *et al*., 2007).Leishmaniasis is mostly found in Asia, Africa, the Mediterranean and South America, with different strains prevalent in different regions causing different clinical manifestations.

Leishmaniasis has 3 main clinical manifestations, which vary in severity and symptoms depending on the infecting species. Visceral leishmaniasis (VL), caused by *L. donovani* or *L. infantum* , patients will suffer from splenomegaly, emaciation, and fever amoungst other symptoms (Choi and Lerner, 2001). *L. donovani* is mainly found in India and Bangladesh and is the main cause of VL. *L. infantum* can cause both VL and CL and is found in the Mediterranean region (Pavli and Mazlou, 2010). The second clinical manifestation is mucocutaneous leishmaniasis (MCL), caused by *L. braziliensis* and its symptoms include lesions at the nasal cavity and mouth which lead to extensive midfacial destruction. The third and most common manifestation is cutaneous leishmaniasis (CL), caused *L. major* or *L. mexicana* where ulcerating skin lesions occur at site of infection (Pavli and Mazlou, 2010). *L. major* and *L. mexicana* both cause CL and is mostly found in South America.

Cutaneous leishmaniasis is the most prevalent form of leishmaniasis and is the least fatal. However, it is a growing concern as more people are being infected with no effective treatment or vaccines, which increases cost to healthcare (Pavli and Maltezou, 2010; Aruleba *et al*., 2020) .This could be accounted for by the poor penetrance of drugs in skin lesions and the role of the skin lesion pathology. Every year 700 000 to 1 million people are diagnosed with CL (Palma *et al*., 2021) and many more are not reported due to being asymptomatic (Mera-Ramírez *et al*., 2017). *L. major* causing CL is prevalent in Syria, South Sudan, Ethiopia, and Afghanistan and is the focus of the study moving forward.

1.3. Drug targets and treatment approaches of cutaneous leishmaniasis

1.3.1 Drugs

Anti-leishmanial drugs that are used to treat leishmaniasis include miltefosine, liposomal amphotericin B and pentavalent antimonials which, all target the *Leishmania* parasite (Osero *et al*., 2020) mainly by attacking parasite replication with varying efficacies (Aruleba *et al*., 2020). Currently there are no approved vaccines against cutaneous leishmaniasis, and the treatments available have high drug failure reports due to drug-resistant parasites and are generally cytotoxic to the host leading to a myriad of side-effects (Aruleba *et al*., 2020).

Taken together, these treatments and the side-effects they cause, such as nausea, renal toxicity, and cardiotoxicity, leaves a need for new or improved approaches to understand the mechanisms between *Leishmania* parasites and their mammalian hosts. Importantly, some people may be infected and not present any symptoms (Mera-Ramírez *et al*., 2017), hence the host pathway must play a role in disease manifestation. Accordingly, this has led to alternate treatment approached termed host-directed therapies (HDTs).

1.3.1. Host- directed therapies

Host-directed therapies (HDTs) use the link between disease and host to create a favourable immune response which ultimately protects the host against infectious and non-infectious agents (Kaufmann *et al*., 2018). HDTs use a range of available drugs that are safe to use and readily available. They can also include nutritional products, like vitamins to enhance immune pathways or by stimulating host immunity (Zumla *et al*., 2016). One of the main objectives of HDTs is to target immune pathways (immunotherapy) within the host or by working with an established drug treatment such as chemoimmunotherapy (Kaufmann *et al*., 2018). Historically, chemoimmunotherapies have been favoured in treatments as they target both the host and the pathogen (whether infectious or not). They also

offer minimal drug resistance, as it is rarely reported that host molecules will develop resistance against HDTs (Munita and Arias, 2016).

Host-directed therapies have been used in conjunction with chemotherapy to combat leishmaniasis (Aruleba *et al*., 2020). When Type 1 T-helper (Th-1) related cytokines were used with immunotherapy, control of leishmaniasis was reported. For instance, treatment with cytokines like interleukin (IL)-12 (IL-12) and interferon-gamma (IFN-γ) reduced leishmaniasis infections caused by *L. donovani* by 47% and 40%, respectively (Murray *et al*., 1995) in murine models. To identify targets for HDTs, there is a need to understand how the host and *Leishmania* parasite interact

1.3.2 *Leishmania* parasite and interaction with model hosts

Due to the underlaying interactions between the murine host and *Leishmania major* parasites, immune response can be either detrimental or beneficial to the parasite thereby promoting resistance or susceptibility, respectively. Hence, another aim of HDTs is to identify any compound or agent that can magnify the oxidative burst of phagocytic cells, such as macrophages or DCs, as well as their phagocytic ability (Murray, 2001). Additionally, HDTs can be combined with chemotherapies to clear *Leishmania* infections by stimulating Th1-related cytokines which, can be used to control disease progression of leishmaniasis in murine hosts.

Table 1: Summary of Th1 vs Th2 response. Host-directed therapies (HDTs) will favour Th1 response because it clears the infection, while trying to avoid eliciting a Th2 reaction from the host immune system to prevent parasite survival in murine models

	Th1 Response	**Th2 Response**
Stimulated by	Proinflammatory cytokines (IL-12, IFN-γ, TNF-α)	Anti-inflammatory cytokines (IL-4, IL-13)
Macrophages	Classically activated	Alternatively activated

Result	Destruction of *Leishmania* parasites and clearing of infection	Formation of necrotic lesions and *Leishmania* parasite survival

1.3.3 Host-immune response to *Leishmania major* infection

Studies have shown that if dendritic cells (DCs) have been induced by IL-4 to produce IL-12 because of the decrease in IL-10, this may lead to a favourable Th1 response, when infected with *L. donovani* (Aruleba *et al*., 2020). This is ironic, as shown in Table 1, IL-4 is associated with eliciting a Th2 response when infected with *L. major* (Hurdayal and Brombacher, 2017). **Table 1** also shows that the killing of intracellular *Leishmania* parasites depends on anti-inflammatory cytokines. The killing occurs because anti-inflammatory cytokines enhance nitrite production via classically activated macrophages (Hurdayal and Brombacher., 2014). Based on the abovementioned information, HDTs seem to have a promising future in treating or co-treating *Leishmania* infections in endemic regions.

There is a strong association of anti-inflammatory cytokines (IL-4, IL-13, and IL-10) with eliciting a Th2 response (Hurdayal *et al*., 2013; Hurdayal *et al*., 2017; Yue *et al*., 2015). Thus, inducing a Th1 response has been favoured by HDTs to clear leishmaniasis as shown by treating with interleukin (IL)-2, -12 and interferon (IFN)-γ (Murray *et al*., 1993; Murray and Hariprashad, 1995; Sundar and Murray, 1995).

It was initially thought that macrophages played minimal roles in host immunity. However, it has been shown that macrophages, derived from myeloid cells, have the power to either protect against or promote disease by directly and indirectly influencing adaptive immune response (Mills., 2015; Roy *et al*., 2015). This relies on the cytokines stimulated such as IL-4 or IL-13. However, disease progression or host protection relies heavily on the polarization of macrophages, which have been divided into two groups: classically (M1) and alternatively activated macrophages (M2) (Govender *et al*., 2018; Guler *et al*., 2015). This difference is

induced depending on the cellular microenvironment signalling cytokines at the time. M1 macrophages are induced by pro-inflammatory cytokines, such as interferon-gamma (IFN-γ) and interleukin-12 (IL-12), thus allowing control over the leishmaniasis infection by stimulating the production of nitric oxide via inducible nitric oxide synthase (iNOS) activation (Dayakar *et al*., 2019). Moreover, alternatively activated macrophages, known as M2 macrophages, are induced by anti-inflammatory cytokines such as IL-4 and IL-13. These are linked to a Th2 response and cause disease progression as illustrated in **Figure 1.2** (Govender *et al*., 2018; Roy *et al*., 2015; Ulusan *et al*., 2020).

Alternatively activated macrophages via Th2 responses, IL-4 or -13 signalling, inhibits iNOS expression, therefore, inhibiting IFN-γ -induced M1 macrophages and induction of Th1 response. The secretion of arginase 1 (Arg), which competes with nitric oxide synthase (iNOS) for catabolism of L-arginine leads to inhibition of M1 macrophage activation and a reduction in Th1 proinflammatory response (Mills, 2015; Sacks and Noben-Trauth, 2002). Thus, allowing parasites to survive as the parasites can use the urea made from arginase (Arg) to grow and replicate (Hurdayal and Brombacher, 2017). In essence, IL-4 counter regulated the expression of IFN-γ, since nitric oxide causes the killing of intracellular parasites due to the induction of M1 macrophages and subsequent induction of Th1 proinflammatory response (Govender *et al*., 2018).

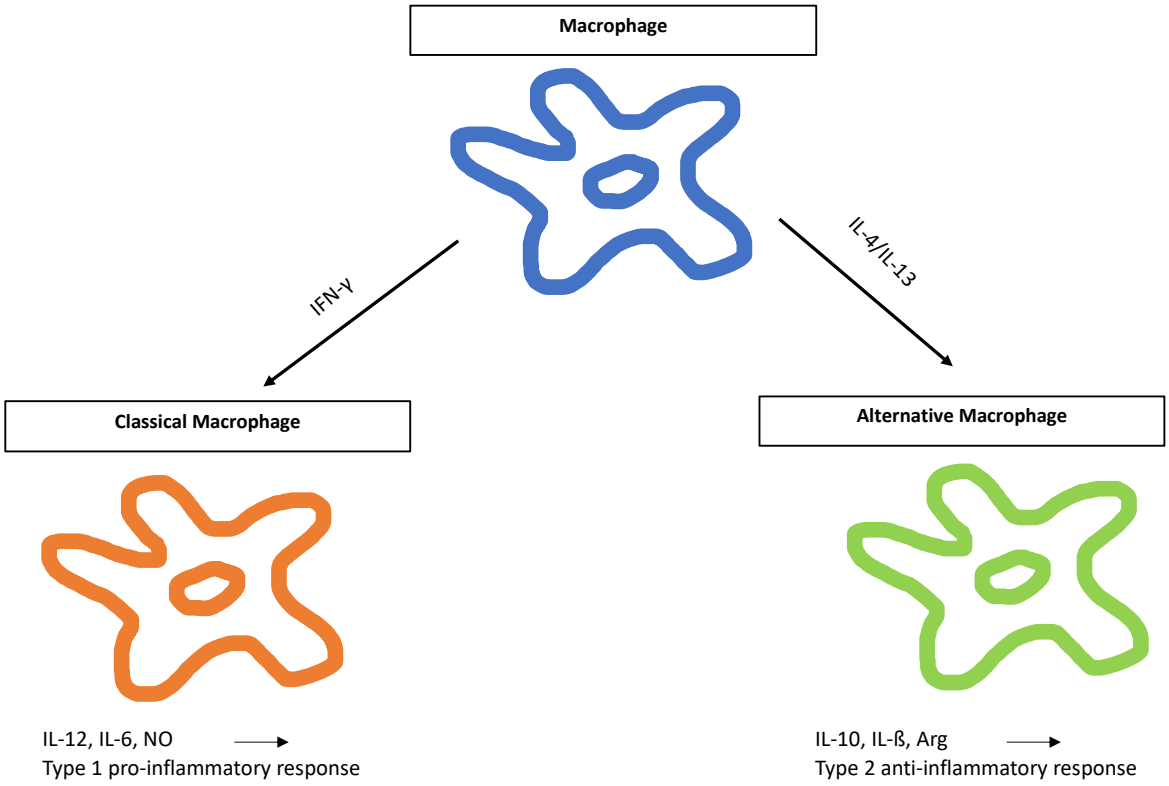

Figure 1.2: Activation of macrophages depends on the internal cell environment and which cytokines are present. Classical activation (M1) is induced by the presence of Type 1 cytokines such as IL-12 and IL-6 which allow for disease control and ultimately healing by upregulating the expression of iNOS. Alternative activation (M2) is induced by the presence of Type 2 cytokines such as IL-4 and IL-13, which allow for disease progression and parasite survival since IL-4 inhibits the induction of M1 macrophages (Mills, 2015; Sacks and Noben-Trauth, 2002).

1.3.4 Interleukin (IL)- 4 and its link to interleukin-1 induced gene-4 (IL-4i1)

Interleukin (IL)-4 is a cytokine that is produced by a Th2 immune response and is signalled via the IL-4 receptor alpha chain (Govender *et al*., 2018). However, it is controversial in the leishmanial context. While studies show it is a critical factor for susceptibility (Kopf *et al*., 1996; Mohrs *et al*., 1999) other studies show that it is dispensable as mice deficient for IL-4 were unable to control susceptibility to CL (Noben-Trauth *et al*., 1996). Notably, these studies used different strains of *Leishmania,* which could have affected the outcome of each experiment. Importantly, IL-4 promotes the differentiation of M2 macrophages **(Figure 2)** which is required for an establishment of CL in murine hosts (Mohrs *et al*., 2000; Sacks and Noben-Trauth, 2002). On the other hand, IL-4 has been shown to act on

dendritic cells (DCs) to instruct IL-12, which stimulates host protection in murine models of CL (Osero *et al*., 2020).

Clearly, IL-4 has distinct roles in cells of the myeloid lineage, depending on which cell it is interacting with. IL-4 has also been responsible for immunoglobulin (Ig) class switching in activated B cells to express IgE instead of IgG4 in humans (Hurdayal and Brombacher., 2017). While IL-4 signalling is responsible for alternatively activated macrophages, IL-4 secretion inhibits IFN-γ induced classically activated macrophages by inhibiting inducible nitric oxide synthase (iNOS) which, ultimately inhibits induction of a type 1 response (Hurdayal and Brombacher., 2017). It can be shown that IL-4 acts antagonistically to IFN-γ (Nelms *et al*., 1999). Apart from T-lymphocytes and macrophages, IL-4 has also been documented in the activation of immunoregulatory enzymes during infection and inflammation (Molinier-Frenkel *et al*., 2019). One such link is between the enzyme interleukin-1 induced gene-4 (IL-4i1) and the cytokine interleukin-4 (IL-4).

When human peripheral blood (B) cells were stimulated by IL-4, the expression of interleukin-4 induced gene-1 (IL-4i1) was activated (Molinier-Frenkel *et al*.,2019). This activation was shown to be achieved via the STAT6 and NF-κB pathways, however, expression is not restricted to B cells as IL-4i1 was also produced by macrophages and DCs when stimulated with IL-4 (Marquet *et al*., 2010).

Concisely, IL-4i1 is part of the L-amino oxidase family (Boulland *et al*., 2007; Molinier-Frenkel *et al*., 2019). This enzyme is vital in the catabolism of phenylalanine, water (H_2O) and oxygen (O_2) to produce phenylpyruvate, ammonia (NH_3) and hydrogen peroxide (H_2O_2) (Cousin *et al*., 2015) (**Figure 1.3**).

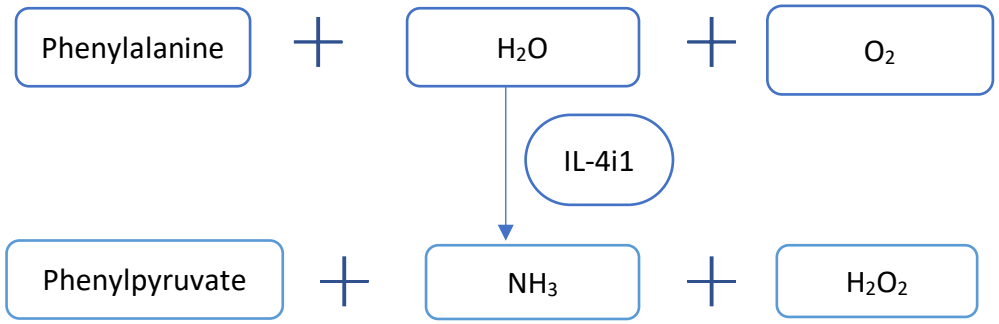

Figure 1.3: Catabolism of the phenylalanine amino acid by IL-4i1. IL-4i1 is an amino acid catabolizing enzyme that produces phenylpyruvate, hydrogen peroxide and ammonia and when catabolizing phenylalanine, water, and oxygen. This catabolism aids in the destruction of parasites by creating an unfavourable environment for *Leishmania* (Molinier-Frenkel et al., 2019).

The catabolism of phenylalanine to produce ammonia and hydrogen peroxide is how IL-4i1 can defend against infections (**Figure 1.3**). This is achieved through various ways. One way is when IL-4i1 induction depletes sources of phenylalanine, which is especially relevant in auxotrophs, such as *Leishmania* (Molinier-Frenkel *et al*., 2019). Additionally, the by-product of the reaction, (hydrogen peroxide) has antiseptic properties (Puiffe *et al*., 2013) which, prevents the growth of disease-causing microorganisms, such as *Leishmania major* parasites. The presence of ammonia also increases the pH of the cell's micro-environment (Puiffe *et al*., 2013) making survival difficult as the environment becomes basic. The expression of *IL-4i1* has been involved in the defense against various infections, such as fungal infections, *Aspergillus fumigatus* (Seddigh et al., 2017), *Candida albicans* (Reales-Calderón *et al.*, 2017), viral infections involving influenza and human immunodeficiency viruses (Anyanwu *et al*., 2018; Baas *et al*., 2006).

IL-4i1 has been seen to effect human T-cells as illustrated in **Figure 1.4.** This is illustrated as a decreased proliferative capacity of human T lymphocytes. It was also recorded that both effector/memory $CD4^+$ and $CD8^+$ T lymphocytes are affected by IL-4i1 expression, in a similar way. This negatively affects proliferation and functions of the T cells as infection can manifest severely (Molinier-Frenkel *et al*., 2019). However, as shown in **Figure 1.4**, IL-4i1 allows for the differentiation of naïve $CD4^+$ T cells into $FoxP3^+$ Treg cells which could have inhibitory effects on

the effector/memory $CD4^+$ and $CD8^+$ cells (Cousin *et al*., 2015). Hence showing the importance of IL4i1 during defense against infectious agents like *Leishmania major*.

1.3.5 *IL-4i1* as a potential host-directed target in cutaneous leishmaniasis (CL)

Hydrogen peroxide has been shown to destroy *Leishmania* parasites (Das *et al*., 2001; Hurdayal and Brombacher, 2017). Thus, the presence of H_2O_2, via catabolism of phenylalanine by IL-4i1 could have beneficial effects for the host in response to *Leishmania major* infection. Moreover, *Leishmania* parasites are auxotrophic, meaning that they cannot produce phenylalanine and must acquire it from the microenvironment to survive (Molinier-Frenkel *et al*., 2019). Hence, the presence of IL-4i1 causes the depletion of phenylalanine and the parasites could starve (Cousin *et al*., 2015). Altogether, these highlight a potential role for IL-4i1 in host protection to CL.

However, a potential role as a host susceptibility factor also exists since, IL-4i1 has been shown to play a key role in M2 macrophage polarization (Yue *et al*., 2015). As described in section 1.2.2, M2 counter-regulates M1 and stimulates a type 2 immune response, thereby promoting the growth of *Leishmania* parasites (Hurdayal *et al*., 2017). Ultimately, this would allow for disease progression. Hence, *IL-4i1* could modulate M2 and parasite survival. Thus, IL-4i1 offers multiple avenues of host immune regulation as an HDT target, during infection with cutaneous leishmaniasis (CL).

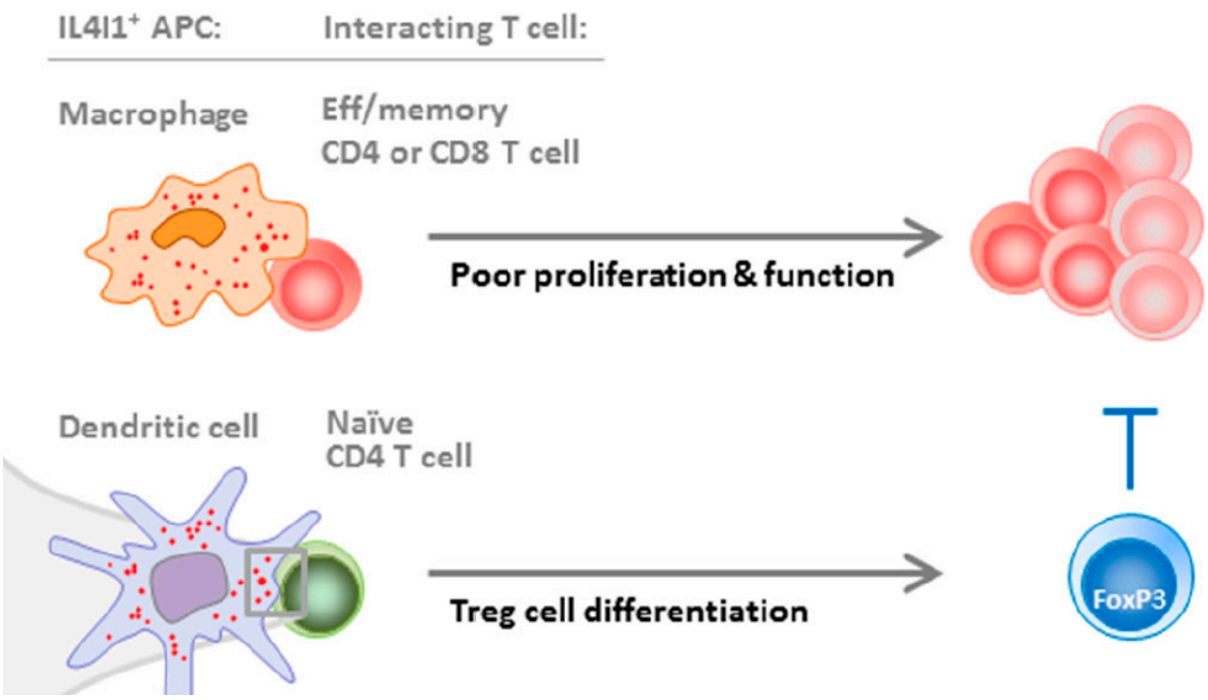

Figure 1.4: Immune response regulated by IL-4i1. Antigen presenting cells like macrophages and DCs produce the amino-acid catabolizing enzyme IL-4i1. They do so when stimulated appropriately and IL-4i1 will interact with the appropriate T cell at the immune synapse. When interacting with effector/memory $CD4^+/CD8^+$ T cells, IL-4i1 will lead to poor proliferation and affects downstream functions of these cells. When DCs interact with naïve $CD4^+$ T cells, this differentiates Treg cells into $FoxP3^+$ cells, which could also have an inhibitory effect on effector T cells (Molinier-Frenkel et al., 2019).

1.4 *In vitro* models to study cutaneous leishmaniasis

Whilst *in vivo* models have been used, *in vitro* models, both murine and human, have also been used to study many diseases especially in the context of specific cell-based mechanistic interactions. One such model is the murine RAW 246.7 cell line which has been used as a primary cell for studying cellular responses against diseases like cutaneous leishmaniasis (Jantsch *et al*., 2015).

The polarisation of leishmaniasis has been a mystery for researchers. By infecting *ex vivo* models such as BALB/c and C57BL/6 mice with *L. major,* it was shown that disease progression and susceptibility were present in BALB/c mice whereas resistance and disease clearance were present in C57BL/6 mice (Bankoti and Stäger, 2012; Egui *et al*., 2018). However, *ex vivo* experiments include the interplay of the host with all immune cells while *in vitro* studies can isolate the immune polarization by investigating individual pathways in potentially, specific

cells. During *Leishmania* infection, macrophages play a critical role in disease outcome as cells that can control infection or cause its progression by virtue of M1 and M2 activation. Thus, *ex vivo* models that utilises macrophage cell-based models may give insights into disease outcome by studying macrophage polarization. In a murine system, this can be achieved by generating bone-marrow derived macrophages (BMDMs) and infecting with *Leishmania.* This process is initiated by stimulating bone-marrow monocytes, which then induce a macrophage phenotype (Heib *et al*., 2021) that is subsequently infected with *L. major*.

The same principles apply to human *in vitro* models, by using human cells more information can be gathered about human immunity. Models like Mono Mac 6 Human monocytic cell lines have been used to understand leishmaniasis (Hansen *et al*., 2011). As seen in Table 2, shows another model, U-937 which has been used by Duque-Benítez *et al*., (2016). However, the use of THP-1 monocytic cell line has long been favoured in leishmaniasis. The THP-1 monocytic cell line was established in 1980 and was derived from the blood of a boy suffering from leukaemia (Tsuchiya *et al*., 1980). It has been preferred for its shorter doubling time. By stimulating THP-1 monocytes with 13-phorbol 12-myristate (PMA), macrophage phenotypes are visible (Chanput *et al*., 2014; Lund *et al*., 2016). THP-1 monocytic cell lines retain functionality, signal pathways and monocyte/macrophage expression markers, giving them an advantage over other cell lines (Lund *et al*., 2016). After differentiation into THP-1-derived macrophages, the macrophages are infected in the same way as the BMDMs and both cell lines are analysed for their cell-based mechanistic interactions.

Importantly, in both models, polarization of macrophages may also be induced by using interferon (IFN)- γ for M1 or interleukin (IL)-4 for M2 macrophages (Chanput *et al*., 2014).

Table 2. Comparison of human *in vitro* cell line used in leishmaniasis studies. THP-1, U-937 and Mono Mac 6 are the most used human *in vitro* cell lines most used in leishmaniasis studies. While they share many characteristics, such as the fact that they are all immortalized, their main difference is the doubling time (Chanput *et al*., 2014)

	THP-1	**U-937**	**Mono Mac 6**
Doubling time	35 hours	72 hours	48 hours
Safe to use	Yes	Yes	Yes
Immortalised	Yes	Yes	Yes
Homogenous genetic background	Yes	No	No

1.5 Aims and objectives

The aim of this study is to characterize the role of *IL-4i1* as a host immunoregulator in cell-based models during infection with *Leishmania major* causing cutaneous leishmaniasis.

The following objectives were set to achieve the above aim:

- Gene-silencing of *IL-4i1* in THP-1-derived macrophage cell line
- Generation of bone-marrow derived macrophages (BMDMs) and confirmation of gene-deletion of *IL-4i1* in BMDMs
- Infection of THP-1-derived macrophages and IL-4i1-deficient BMDMs with *L. major.*
- Characterisation of parasite burden and cellular immune response post-*L. major* infection of *IL-4i1*-silenced THP-1-derived macrophages and *IL-4i1*-deficient BMDMs

2. Materials and Methods

2.1 Ethics Statement

All procedures described in this study were performed under strict accordance with the recommendations of the South African national guidelines (SANS 10386:2008) and the Animal Research Ethics Committee (AEC) based at the Faculty of Health Sciences, University of Cape Town (UCT). All protocols involving mice were approved by the Animal Research Ethics Committee permit numbers: 019/001. Biosafety protocols were also approved by Science Faculty Biological Safety Committee, BSC005_2019. South African Veterinary Council authorisation number AR19/17680.

2.2 Mice

Mice deficient for *IL4i1* on a BALB/c background were purchased from Lexicon Pharmaceuticals Inc., USA, and were created by using the pKOS-17 target vector to transfect BALB/c embryonic stem cells. Through homologous recombination, the vector replaced exons 2-8, which begin at the start site for the *IL4i1* gene. The process is in-frame with lac-Z and neo cassettes. Mice were grouped as either IL-41-deficient ($IL4i1^{-/-}$) or wildtype ($IL4i1^{+/+}$). All the mice were housed in the Research Animal Facility (RAF) of the Health Science Faculty, UCT. The cages were individually ventilated and were kept in specific-pathogen free conditions with a regular supply of food and water. The mice were sex- matched and used for experiments at 8 weeks old (Hlaka *et al*., 2021).

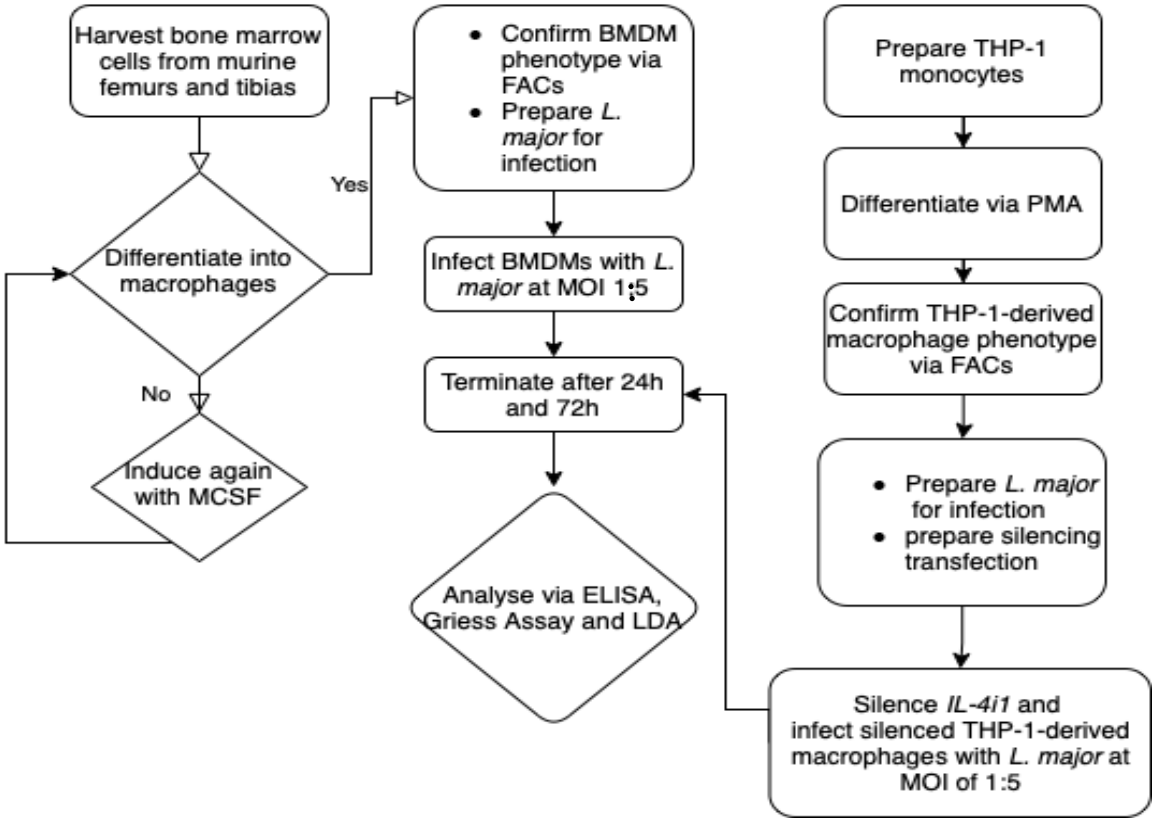

Figure 2.1: General methodology followed throughout this study. Overview of methods used showed via flow diagram to clarify how bone-marrow derived macrophages (BMDMs) were differentiated, infected, and analysed. Flow diagram of THP-1-derived macrophages and their differentiation, infection, and analysis.

2.3 Preparation of *Leishmania major LV39* parasites from frozen stocks

Leishmania major LV39 (MRHO/SV/59/P strain) stocks, $2x10^7$ parasites in 10% v/v dimethyl sulphoxide (DMSO) (Sigma-Aldrich, USA) and 90% fetal calf serum (FCS) (Thermofisher Scientific, USA) were thawed at room temperature and resuspended in 10x volume of 1x phosphate buffered saline [137 mM NaCl, 2.7 mM KCl, 10 mM Na_2HPO_4, 1.8 mM KH_2PO_4] (PBS), pH 7.4 and pelleted at 3000 revolutions per minute (rpm) for 10 minutes at 23°C. The resulting pellet was then resuspended in 10 ml 1x PBS and centrifuged as above to pellet the pure parasites. Following which ,the parasite pellet was resuspended in 5 ml M199 media supplemented with 10% FCS and 1% PenStrep [50 U/ml penicillin; 50 μg/ml streptavidin] (hereafter referred to as cM199) and transferred to a 25 cm^3 (T25) tissue culture flask (SPL Life Sciences, Korea). The T25 flask was incubated at

26°C and when viable growth was evident, another 5 ml of cM199 was added. These *in vitro* parasite cultures were maintained by weekly subculturing 1:50 *L. major* LV39 into a new T25 with 10 mls cM199 and incubated at 26°C.

2.3.1 Preparation of *L. major* culture for *in vivo* infection of BALB/c mice

L. major in vitro cultures were used in preparation for infection of BALB/c. The promastigotes were transferred to a 50 ml sterilin (SPL Life Sciences, Korea) and pelleted at 3000 rpm for 10 minutes at 23°C. Following which, the parasite pellet was resuspended in 1x PBS and washed twice by centrifugation as above. Subsequently, the pellet was resuspended in 1 ml 1x PBS. 1% of the pellet suspension was diluted with 4% paraformaldehyde to fix the parasites onto the Neubauer haemocytometer for counting. A growth curve was prepared by subculturing $1x10^7$ parasites/ml in 10 mls cM199. Parasites were counted daily, and numbers were recorded as an exponential curve (Mohrs *et al*., 1999). By day 6, stationary phase was reached, and the parasites were centrifuged at 3000 rpm for 10 minutes at 23°C. Thereafter, parasites were washed twice in 1x PBS after which they were fixed with 4% paraformaldehyde and counted. The desired concentration for infecting BALB/c mice in the footpads was $2x10^6$ parasites/50 μl. Before infections, mice were anesthetized with 12% ketamine and 8% xylavet in 1x PBS at a dose according to the weight of each mouse (10 μl/gram).

2.3.2 Preparation of *L. major* parasites for *in vitro* infection

At 8 weeks post *L. major* infection in BALB/c mice, animals were euthanized by halothane gas and cervical dislocation. *L. major* amastigotes from the infected footpad were extracted using an insulin syringe containing 100 μl of 1x PBS to aspirate the parasites. The parasite solution was subsequently centrifuged at 3000 rpm for 5 minutes at room temperature after adding 4.9 ml of 1x PBS, bringing total volume to 5 mls. Following which, the pellet was resuspended in 1 ml of cM199, transferred to a T25 (SPL Life Sciences, Korea) with 9 ml of cM199 and incubated

at 26°C in a low-temperature incubator for differentiation into stationary-phase promastigotes. Promastigotes were then prepared for subsequent infection experiments in bone-marrow derived macrophages (BMDMs) or THP-1-derived macrophages as in Section 2.3.1 and as shown in **Figure 2.1**

2.4 Differentiation, stimulation, and infection with *L. major* of bone-marrow derived macrophage (BMDMs)

To differentiate bone-marrow cells to bone-marrow derived macrophages (BMDMs), bone marrow monocytes were isolated from both gene-deficient BALB/c mice ($IL4i1^{-/-}$) and littermate controls ($IL4i1^{+/+}$) at 8 weeks old. Isolation of bone-marrow monocytes was performed as described by Heib *et al*. (2021). Briefly, bone-marrow cells were pelleted from the tibia and femurs from both animals into Eppendorf tubes. These Eppendorf tubes were held by a second Eppendorf tube, which contained 100 μl of Plutznik media. The Eppendorf 'system' was centrifuged at 600 rpm for 2 minutes. Bone marrow monocytes were collected in the bottom Eppendorf tube and counted using blue tryphan exclusion. Differentiation to BMDMs was performed as described elsewhere Lutz *et al*. (1999). This was completed in 15 ml star petri dishes (Cambridge Environmental, Canada) which contained Plutznik media (Dulbecco's Modified Eagle medium (DMEM) supplemented with 10% FCS, 5% horse serum, 30% L929 cell-conditioned medium containing macrophage colony-stimulating factor (M-CSF), 2 mM L-glutamine, 2 mM sodium pyruvate, 0.1 mM 2-mercaptoethanol and Penstrep [100 U/ml; 100 μg/ml]). After 5 days, an additional 5 ml (half volume) of Plutznik media was added to replenish the cells. On day 10, BMDMs were detached from the petri dishes using 0.025% trypsin-ethylenediamine tetra-acetic acid (EDTA) diluted in 1x PBS. Subsequently, the BMDMs were washed and pelleted to be counted using trypan exclusion in a Neubauer counting chamber. $2.5x10^5$ cells/well were seeded in a 96-well- U bottom plate (SPL Life Sciences, Korea) in complete DMEM (DMEM, 10% FCS, 1% Penstrep [100 U/ml; 100 μg/ml]) (cDMEM). BMDMs were left in a humidified incubator (37°C and 5% CO_2) for 3 hours. Following which, BMDMs were either stimulated with 1000 U/ml interferon-gamma (IFN-γ) (BD

Bioscience, Catalogue number 554587, [500 ng/μl]) or 1000 U/ml interleukin-4 (IL-4) (BD Bioscience, Clone number 11B11, [2 μg/ml]) or left unstimulated for 24 hours in a humidified incubator. Subsequently, BMDMs were prepared for flow cytometry analysis and infected with *L. major* promastigotes, prepared as in Section 2.3.2, at MOI of 1:5 for 24 and 72 hours, respectively.

2.4.1 Flow cytometry analysis of bone-marrow derived macrophages or THP-1-derived macrophages

Bone-marrow derived macrophages or THP-1-derived macrophages were first detached from each well using 1 ml of 0.025% trypsin-ethylenediamine tetra-acetic acid (EDTA) diluted in DMEM (all Thermofisher Scientific, USA). After adding trypsin-EDTA to each well, the BMDMs or THP-1-derived macrophages were left to incubate in a humidifier (37°C and 0.5% CO_2) for 20-30 minutes. Progress of detachment was confirmed via light microscopy and once detachment was completed, trypsin-EDTA was deactivated by adding 1 ml of cDMEM or cRPMI to each well. Each well, containing 2 ml of solution, was then collected in a 50 ml sterilin (SPL Life Sciences, Korea) and pelleted at 1300 rpm for 5 minutes. BMDMs or THP-1-derived macrophages were then resuspended in 1 ml of prewarmed cDMEM or cRPMI and counted using trypan blue exclusion (Sigma-Aldrich, Germany) on a Neubauer Counting Chamber. $2x10^6$ cells/ml were seeded in a 96-well v-bottom plate (Nalge Nunc International, USA) and pelleted at 1300 rpm for 5 minutes at 4°C. Following which, the supernatant was discarded, and the cells were resuspended in 50 μl FACS buffer (0.5% BSA in 1X PBS, pH 7.4) supplemented with 1% rat-serum and 1% Fc gamma receptor blocker (2.4G2) and fluorescently labelled antibodies for extracellular staining (**Figure 2.1**). Murine antibodies included CD11b-Per-CP and F4/80-allophycocyanin (APC). While human antibodies included CD14-BV650, CD16-Pe-Cy5 and CD64-Pe-Cy7 (Appendix Table S1 and S2). The Nunc plate was covered in foil and incubated at 4°C for 20 minutes for staining to occur. Following the incubation, 150 μl of FACS buffer was added to each well and the plate was pelleted as above. After pelleting, the supernatant was discarded, and the pellet was resuspended in 50 μl of FACS

buffer until acquisition. Acquisition was completed on BD LSR Fortessa Machine (BD Biosciences, USA) and the data was analysed via FlowJo software (Treestar, USA).

2.5 Growth and maintenance of THP-1 monocytes

The human monocytic cell line, THP-1 ATCC#TIB-202 cells were received as a kind donation from Professor Frank Brombacher, Institute of Infectious Diseases and Molecular Medicine, University of Cape Town, South Africa. $4x10^6$ cells/ml were thawed in a 37°C water bath and aspirated into 10 mls of preheated (at 37°C) Roswell Park Memorial Institute- 1640 (RPMI-1640) media supplemented with 10% fetal calf serum (FCS), penicillin streptomycin (PenStrep) ([50 U/ml] and [50 µg/ml]) and ß-mercaptoethanol [0.05 mM] (all from Thermofisher Scientific, USA), hereafter referred to as complete RPMI (cRPMI). Once aspirated, cells were pelleted at 1300 revolutions per minute (rpm) for 5 minutes. Thereafter the supernatant was discarded, and the pellet was resuspended in another 10 mls of cRPMI and pelleted again. This washing process was repeated twice more. After the final wash, cells were resuspended in 5 mls of cRPMI and 10 µl were used to count viable cells using trypan blue exclusion (Sigma-Aldrich, Germany). Cells were counted using the Neubauer counting chamber and seeded at $1x10^5$ cells/ml in 20mls of cRPMI in T75 flasks (Biosmart, South Africa). Cells were kept horizontally in a humidified incubator (37°C and 5% CO_2). Cells were counted again only on day 3. Confluency was reached by day 5 or when cells were at $1x10^6$ cells/ml and split at a ratio of 1:1 to allow for acclimatization to growth conditions (**Figure 2.1**).

2.5.1 Differentiation of THP-1 monocytes to THP-1-derived macrophages using phorbol 12-myristate 13-acetate

When THP-1 monocytes reached $1x10^6$ cells/ml in T75 flask (Biosmart, South Africa) viability was determined using trypan blue exclusion (Sigma-Aldrich, Germany) to seed cells for differentiation to macrophages (**Figure 2.1**). Differentiation was performed using phorbol 12-myristate 13-acetate (PMA)

(Thermofisher Scientific, USA) at [60 ng/µl] in 3 mls of cRPMI. THP-1 monocytes were pelleted at 1300 rpm for 5 minutes and subsequently resuspended in 1 ml of prewarmed cRPMI. Trypan blue exclusion as well as a Neubauer Counting Chamber were used to count the cells, which were then seeded at $2x10^6$ cells/ml. Subsequently, $2x10^6$ cells were added to each well of a sterile, tissue culture grade 6-well plate (Biosmart, South Africa), followed by 1 ml of PMA [20 ng/µl] and 1 ml of cRPMI was added to bring final volume to 3 mls in each well. Cells were left to incubate in a humidifier (37°C and 5% CO_2) for 48 hours. After 24 hours, cells were checked using light microscopy to confirm macrophage morphology and adherence. Subsequently, at 48 hours the PMA-media was aspirated and replaced with 3 mls of preheated cRPMI to allow for a 24-hour rest period.

2.5.2 Lipofectamine RNAiMAX™ Transfection of THP-1-derived macrophages using Silencer Select™ small interfering RNAs

THP-1-derived macrophages were first detached as described in sub-section 2.5.2. THP-1-derived macrophages were seeded at $4x10^4$ cells/ml in 96-well plate (Biosmart, South Africa) for 3 hours to rest and attach prior to transfection. After 3 hours, THP-1-derived macrophages at 50% confluency, were ready for transfection. The Lipofectamine RNAiMAX™ (Life Technologies, USA) was used according to the manufacturer's instructions. Briefly, small interfering RNAs (siRNAs) (Life Technologies, USA) for each gene were prepared by creating a 100 µM stock using nuclease- free water. A 10 µM working stock was subsequently prepared and aliquoted for later uses. In separate Eppendorf tubes, Lipofectamine RNAiMAX™ (Life Technologies, USA) and the siRNAs were diluted in serum-free RPMI-1640 media (Thermofisher Scientific, USA) at a ratio of 1:16 (Lipofectamine:RPMI-1640) and ratio of 1:50 (siRNA:RPMI-1640) in a final volume of 25 µl, respectively. The preparation of the siRNA-Lipofectamine RNAiMAX™ complex was performed by adding the diluted lipofectamine to the diluted siRNA. At this point the complex was left to incubate at room temperature for 10 minutes.

At the point of transfection, cRPMI was aspirated from THP-1-derived macrophages in the 96-well plate and replaced with 100 µl RPMI after which, 10 µl of siRNA- Lipofectamine RNAiMAX^{TM} complex were added to each well and left to incubate in a humidified incubator (37°C and 0.5% CO_2) for 24 hours. Following the incubation period, the *IL-4i1* silenced THP-1-derived macrophages were prepared for either RNA extraction by replacing the transfection media with 300 µl of RNA lysis buffer (Zymo Research Kit- Inqaba, South Africa) to lyse the cells. After which, the *IL*-4i1 silenced-THP-1-derived macrophages were stored at -20°C for RNA extractions and supernatants were collected for downstream analysis.

2.5.3 *In vitro* infection of THP-1-derived macrophages using *Leishmania major* LV39

Before infecting, gene-silenced- THP-1-derived macrophages and the control was checked using light microscopy for adherence. Following which the same protocol was followed as in section 2.3.2. At the same time, the parasite growth would have reached stationary phase and thus THP-1-derived macrophages were infected at a multiplicity of infection of 1:5 ($1x10^5$ cells:$5x10^5$ parasites) in a 96-well plate (SPL Life Sciences, Korea), where the THP-1 derived macrophages were added to the wells first followed by the parasites (**Figure 2.1**). Subsequently, the 96-well plates were incubated for 24 and 72 hours in a humidified incubator (37°C and 5% CO_2).

2.6 Viability of THP-1-derived macrophages during *L. major* infection

To determine the viability of THP-1-derived macrophages during infection with *L. major*, a colorimetric 3-(4,5-dimethylthizolyl-2-)-2,5-diphenyltetrazolium bromide (MTT) assay was performed (Yue *et al*., 2015). THP-1-derived macrophages were seeded at $1x10^5$ cells/100 µl in replicates for each time point (0 hour, 24 hours, 72 hours, and 6 days) on separate 96-well plates (SPL Life Sciences, Korea). MTT was dissolved to 5 mg/ml in serum free RPMI-1640. At each time point, the cRPMI was removed and cells were washed with 1x PBS and the MTT solution was added. Subsequently, the plate was incubated in a humidifier for 2 hours following

which the plate was centrifuged at 200 rpm for 10 minutes. The MTT solution was then discarded and an equal volume of dimethyl sulphoxide (DMSO) was added. The plate was incubated at room temperature until all the crystals dissolved and the optical density was then measured at 570 nm using a microplate reader.

2.7 Quantification of internalized *Leishmania major* amastigotes via endpoint polymerase chain reaction (PCR)

Infections of THP-1-derived macrophages were terminated after 24 or 72 hours when the supernatant was aspirated from each well. Subsequently, samples were prepared for deoxyribonucleic acid (DNA) extractions through the addition of 50 µl of a 10% sodium dodecyl sulphate solution (SDS) (Sigma-Aldrich, Germany). This detached the THP-1-derived macrophages from the wells and was mixed with 450 µl of DNA lysis solution [10 mM EDTA, 40 mM sodium chloride (NaCl)] (All from Sigma-Aldrich, Germany). Following which, the contents of the wells were transferred to labeled 1.5 ml Eppendorf tubes where DNA of internalized parasites was extracted.

Genomic DNA (gDNA) extraction protocol followed was established by Aljanabi and Martinez (1997) with some modifications. The DNA extraction was performed by incubating each sample with 20 µl of Proteinase K [20 mg/ml] (Thermofisher Scientific, USA) at 56°C for 2 hours. Following which, the incubation was terminated by adding 225 µl of a saturated salt solution [5 M NaCl] and the samples were further incubated at room temperature for 1 hour. Samples were then pelleted at 10000 revolutions per minute (rpm) at 4°C for 10 minutes. The clear supernatant containing the DNA was then transferred to a new 1.5 ml Eppendorf tube and pelleted again at the same conditions. The supernatant was then transferred again before 1 ml of 35% isopropanol (Merck, Germany) was added to each sample and left overnight at -20°C to allow for DNA precipitation. On the following day, the samples were pelleted as before except for 20 minutes. The supernatant was then discarded, and the pellet was resuspended in 1 ml of 70% ethanol (Merck, Germany) and pelleted again. The samples were then airdried for 1-2 hours before

being dissolved in 30 µl TE buffer [10nM Tris; 1 mM EDTA; ph8] (Sigma-Aldrich, Germany). The dissolved DNA was eluted overnight at -20°C before quantitation using the Nanodrop ND1000 (Thermofisher, USA).

Quantitation of DNA showed the concentration of each sample and its absorbance ratios by confirming the A260/280 ratios. Gel electrophoresis was used to confirm DNA integrity by dissolving 1.5% w/v agarose in 1x Tris-borate EDTA (TBE) buffer and waiting for the gel to set. 10 ng of gDNA was loaded with 6x loading dye (Thermofisher Scientific, South Africa) and run at 100 V using a Bio-Rad Powerpack (Lasec, South Africa) for 30 minutes. Following DNA integrity confirmation, a polymerase chain reaction (PCR) specific to kinetoplast DNA (kDNA) on *L.major* was performed. The PCR was standardized to 2 ng/µl in each reaction to allow for accurate quantification of band intensities. kDNA specific primers for a 120-base pair (bp) fragment were used. Forward primer: 5'-CCT ATT TTA CAC CAA CCC CCA GT-3' and reverse primer: 5'-GGG TAG GGGG CGT TCT GCG AAA-3' (Ivens *et al*., 2005) (IDT, South Africa) and the PCR conditions were as follows: initial denaturation at 94°C for 4 minutes followed by 25 cycles of denaturation at 94°C for 1 minute, annealing at 58°C for 30 seconds, elongation at 72°C for 30 seconds and a final extension at 72°C for 10 minutes before holding the reaction at 4°C for 10 minutes. Briefly, 2 ng/µl of DNA was used in a mix with 0.2 µM forward and reverse primers, 1.5 mM $MgCl_2$, 0.2 mM of each deoxynucleotide triphosphate and 0.2 units of Taq DNA polymerase (KAPA Taq PCR Readymix KK1024, KAPA Biosystems, USA) in a final volume of 10 µl. PCR was performed on an XP thermal cycler (Bioer Technology, China). To visualize kDNA amplification 10 µl of the PCR product was run at 100 volts for 30 minutes on a 1.5% [w/v] agarose gel stained with 5 µg/ml ethidium bromide in 1x Tris-EDTA buffer. The final products were visualized on the Bio-Rad Molecular Imager® Gel Doc™ XR+ (Qiagen, South Africa) using built-in software that captured the gel image. Band intensities were quantified using ImageJ analysis (National Institute of Health, USA). The positive control used was pure *L. major* gDNA at 2 ng/µl,

amplified as above to determine the relative expression levels of internalized kDNA.

2.8 Quantification of *L. major* parasite burden via limiting dilution assays

Once infection of IL4i1-silenced-THP-1-derived macrophages was terminated after 24 and 72 hours respectively, a solution of filtered and warmed 0.016% SDS was made in RPMI-1640 (SDS-RPMI) (both Thermofisher Scientific, USA). This method was adapted from Parihar *et al*. (2016) Briefly, the supernatants from the designated wells were aspirated and stored in Eppendorf tubes to be used for alternative analysis. Following which, 100 µl of the SDS-RPMI solution was added to the exposed gene-silenced-THP-1-derived macrophages in each well and was incubated in a humidified incubator (37°C and 5% CO_2) for 2-3 minutes to allow for non-internalized parasites to be lysed. Subsequently, the solution was aspirated and replaced with another 100 µl of SDS-RPMI solution and incubated for 30 minutes which allowed for the gene-silenced-THP-1-derived macrophages to be lysed and to release the internalized parasites. The gene-silenced-THP-1-derived macrophages were monitored after 15 minutes. Once the 30 minutes were over, 150 µl of 17% FCS in RPMI-1640 (FCS-RPMI) solution was added onto the SDS-RPMI solution in each well. Simultaneously, 100 µl of FCS-RPMI solution was added into all wells in a new 96-well plate (SPL Life Sciences, Korea) except for the first row. In the first row of the new plate, 200 µl of the parasite solution was added and a 1:2 dilution was performed between the rows while the contents of each well was thoroughly mixed. The plates were then wrapped in foil and incubated at 26°C for 7 days which allowed for the differentiation of amastigotes to promastigotes. After 7-day incubation, the number of parasites were counted in each well using light microscopy.

2.9 Quantitative- polymerase chain reaction

Expression of *IL4i1* in THP-1-derived macrophages and bone-marrow derived macrophages (BMDMs) were analysed by quantitative PCR (qPCR). *IL4i1*-silenced-THP-1-derived macrophages or BMDMs were detached from the plates

following sub-section 2.5.2. Briefly, total ribonucleic acid (RNA) was extracted as per manufacturer's instructions by Zymo- RNA Extraction Kit (Inqaba, South Africa). RNA was standardized and reverse transcribed according to manufacturer's protocol using the Tetro-cDNA synthesis kit (Celtic Diagnostics, South Africa). Real time PCR was done using the SensiFAST SYBR No-ROX qPCR Kit (Celtic Diagnostics, South Africa) on the Qiagen Rotor-Gene Q (Qiagen, South Africa). Primers for human *IL4i1*: Forward: 5'-CCA AGA CCC CTT CGA GAA ATG-3', reverse: 5'- GCC TCG GCG AAG CTG AGA T-3' (Yue *et al*., 2015) (White Sci, South Africa). Primers for murine *IL4i1*: Forward: 5'-ATT CCC CAG AGG ACA TCT ACC A-3', reverse: 5'- CTG TAC CGG AGT CTA TCG CTC A -3' (Hlaka *et al*., 2021) (White Sci, South Africa). Messenger RNA (mRNA) expression levels were quantified via relative quantification by normalising to either human *GAPDH* or *18S* or murine *HPRT* using the $2^{-\Delta\Delta Ct}$ method (Schmittgen and Livak, 2008).

2.10 Griess assay

Cell-supernatants from *L. major* infected bone-marrow derived macrophages, *IL4i1*-silenced-THP-1-derived macrophages and THP-1-derived macrophages were used to quantify nitrite production as a proxy for iNOS activity (Guler *et al*., 2015). Briefly, 1 mM of $NaNO_2$ was diluted 1:2 in either DMEM or RPMI in a 96-well flat-bottom plate (SPL Life Sciences, Korea). 50 μl of supernatants were added to respective wells where 25 μl of Griess Reagent 1 (1% sulphanilamide in 2.5% phosphoric acid) was subsequently added in each well followed by a 5 minute incubation at room temperature in the dark. After the incubation an equal volume of Griess Reagent 2 (0.1% naphthyl-ethylenediamine in 2.5% phosphoric acid) was added to each well. Again, the plate(s) was incubated as above until a distinctive pink colour develops across the wells designated for the standard. The optical density of the samples was then measured at 540 nm on a microplate reader. The data was analysed using the SoftMax pro software (Molecular Devices, Germany).

2.11 Cytokine Enzyme-linked Immunosorbent assay (ELISA) analysis

Cytokine secretion from infected BMDMs (section 2.4) and infected *IL4i1*-silenced-THP-1-derived macrophages (section 2.5.3) were analysed via sandwich ELISA as described by Govender *et al*. (2018). Briefly, supernatants were aspirated and collected from all samples and stored at -20°C until analysis. Meanwhile, 96-well plates (SPL Life Sciences, Korea) were coated with primary coating antibodies (Abs) for the cytokines of interest (Appendix Table S3), all diluted 1:500 in carbonate coating buffer (1.5 mM $NaCO_3$, 35 mM $NaHCO_3$ and 71 mM NaCl, pH 9.5) and incubated at 4°C overnight. The following day, the plates were washed 4 times in washing buffer and were blocked with blocking buffer (2% BSA) for 2 hours at 37°C. Subsequently, the plates were washed again as above and the supernatants as well as the recombinant standards for murine and human IL-10 and IL-12 were added to their designated wells and diluted 1:3 after which, the plates were incubated at 4°C overnight. On the following day, the plates were washed as above and the biotinylated secondary anti-mouse and anti-human antibodies were diluted 1:1000 and added to the specific wells. The plates were then incubated at 37°C for 3 hours. Following the incubation, the plates were washed 5 times as above and alkaline phosphatase (AP) labelled streptavidin substrate [1:1000] was added to all plates which were then incubated for another hour at 37°C. These plates were subsequently developed by adding 4-Nitrophenyl phosphate ([1 mg/ml] PNP in AP substrate buffer (9.7% $C_4H_{11}NO_2$, 0.02% NaN_3 and 0.8% $MgCl_2.6H_2O$, pH 9.8)) and left to incubate for 15 minutes in the dark at room temperature. Absorbance was read at 405 nm using a microplate reader.

2.12 Statistical Analysis

All statistical analyses were done using GraphPad Prism v9 (GraphPad Software, USA). The data were calculated as mean ± standard error or the mean (SEM). Statistical analysis was calculated using relevant t-tests between 2 groups. A one-way Analysis of Variance (ANOVA) was used when comparing more than 2 groups with a Bon-feroni post-test used. Significance was defined as *, $p < 0.05$; **, $p < 0.01$; ***, $p < 0.001$; ****, $p < 0.0001$.

3. Results

3.1 Absence of *IL4i1* expression in bone-marrow derived macrophages from *IL4i1*-deficient BALB/c mice and controls

Bone marrow-derived macrophages (BMDMs) were generated from bone marrow monocytes of IL4i1$^{+/+}$ and IL4i1$^{-/-}$ BALB/c mice using granulocyte-macrophage colony-stimulating factor (GM-CSF)-expressing cell line as described by *Guler et al*. (2015). Following 10 days of differentiation, macrophage differentiation was confirmed by flow cytometry, gating on cells double positive for CD11b and F4/80 **(Figure 3.1 A-F)**. Importantly, macrophage differentiation was equivalent between both strains of mice, as shown by 94% CD11b^{+}F4/80^{+} in IL4i1$^{+/+}$ **(Figure 3.1 C)** and 97.3% CD11b^{+}F4/80^{+} in IL4i1$^{-/-}$ mice **(Figure 3.1 F**). Following BMDM generation, we sought to confirm the absence of *IL4i1* expression in IL4i1$^{-/-}$ relative to IL4i1$^{+/+}$ mice. Efficient deletion of *IL4i1* was confirmed in IL4i1$^{-/-}$ using gene specific primers via qPCR using the $2^{-\Delta\Delta Ct}$ method and using *HPRT* as the housekeeping gene **(Figure 3.1 G**).

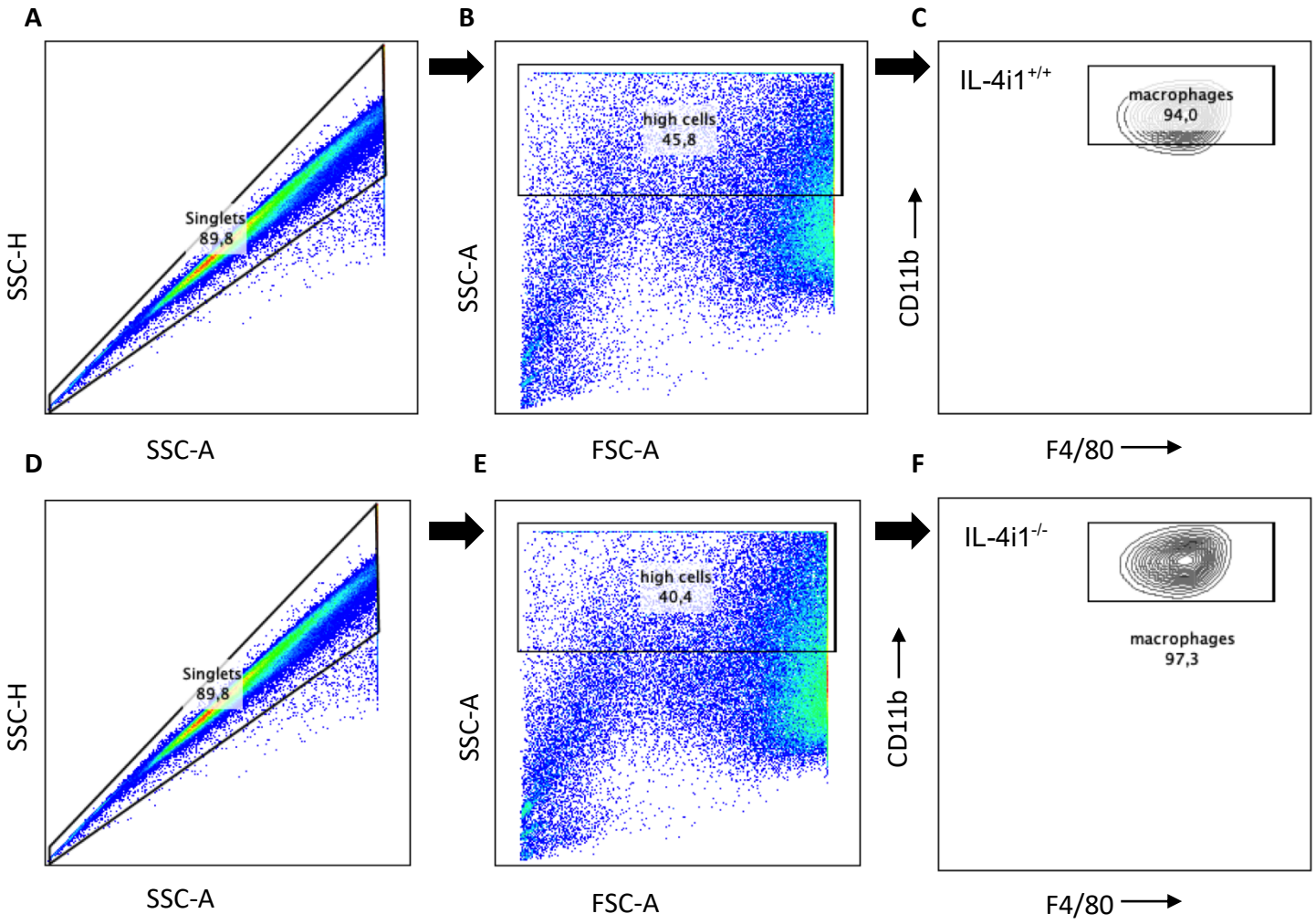

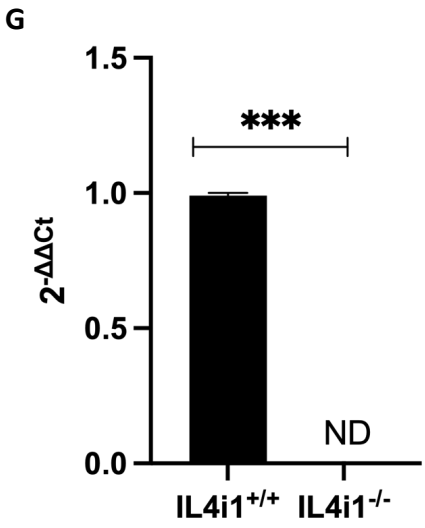

Figure 3.1. Generation of bone marrow-derived macrophages from IL4i1$^{-/-}$ and IL4i1$^{+/+}$ BALB/c mice. Bone marrow cells were isolated from femurs of both IL4i1$^{-/-}$ and IL4i1$^{+/+}$ mice and differentiated into bone marrow-derived macrophages. **A)** Macrophage differentiation was confirmed by flow cytometry using the same gating strategy and by staining for CD11b and F4/80 in **A-C)** IL4i1$^{+/+}$ and **D-F)** IL4i1$^{-/-}$ mice. **G)** Efficient deletion of *IL4i1 expression* was confirmed using qPCR and compared to *HPRT* as the housekeeping gene. Relative expression was calculated using the $2^{-\Delta\Delta Ct}$ method. Statistical significance was calculated using a non-parametric t-test where *** is $p<0.001$.

3.2 Absence of IL-4i1 promotes control of parasite replication during *Leishmania major* infection of BMDMs generated from IL-4i1$^{-/-}$ mice relative to BMDMs generated IL-4i1$^{+/+}$ mice

Bone-marrow derived macrophages (BMDMs) were seeded on day 1 at 2.5x10^5 cells/ml **(Figure 3.2 B**). Once *L. major* promastigotes reached stationary phase on day 5 (**Figure 3.2 A)**, BMDMs were infected with parasites at a multiplicity of infection (MOI) of 1:5 (cells: parasites). After 3 hours, BMDMs were stimulated with 1000 U recombinant mouse IFN-γ and IL-4 to steer the BMDMs towards classical (M1) or alternative (M2) activation **(Figure 1.2)**, respectively, as previously described (Yue *et al*., 2015). At 24hr and 72hr post-infection, parasite burden was analysed using limiting dilution assays (LDAs) (**Figure 3.2 C-D)**. At 24h (**Figure 3.2 C**) and 72h (**Figure 3.2 D**), the IFN-γ stimulated BMDMs from IL-4i1 $^{+/+}$ mice had a higher parasite burden relative to IL-4i1$^{-/-}$ mice **(Figure 3.2 D).** In contrast, IL-4 stimulated BMDMs had reduced burden but not significant, significance between IL4i1$^{-/-}$ mice and IL4i1$^{+/+}$ mice.

Overall, at 24h and 72h, both IL-4 and IFN-γ stimulated BMDMs from IL-4i1$^{-/-}$ mice had a reduced parasite burden relative to IL-4i1$^{+/+}$ mice with significance seen at 24h. This suggests that IL-4i1 may not be independently modulated by M1 and M2 activation because parasite burden, indicated as a reduction in both IFN-γ and IL-4 stimulation but expression itself permits parasite replication.

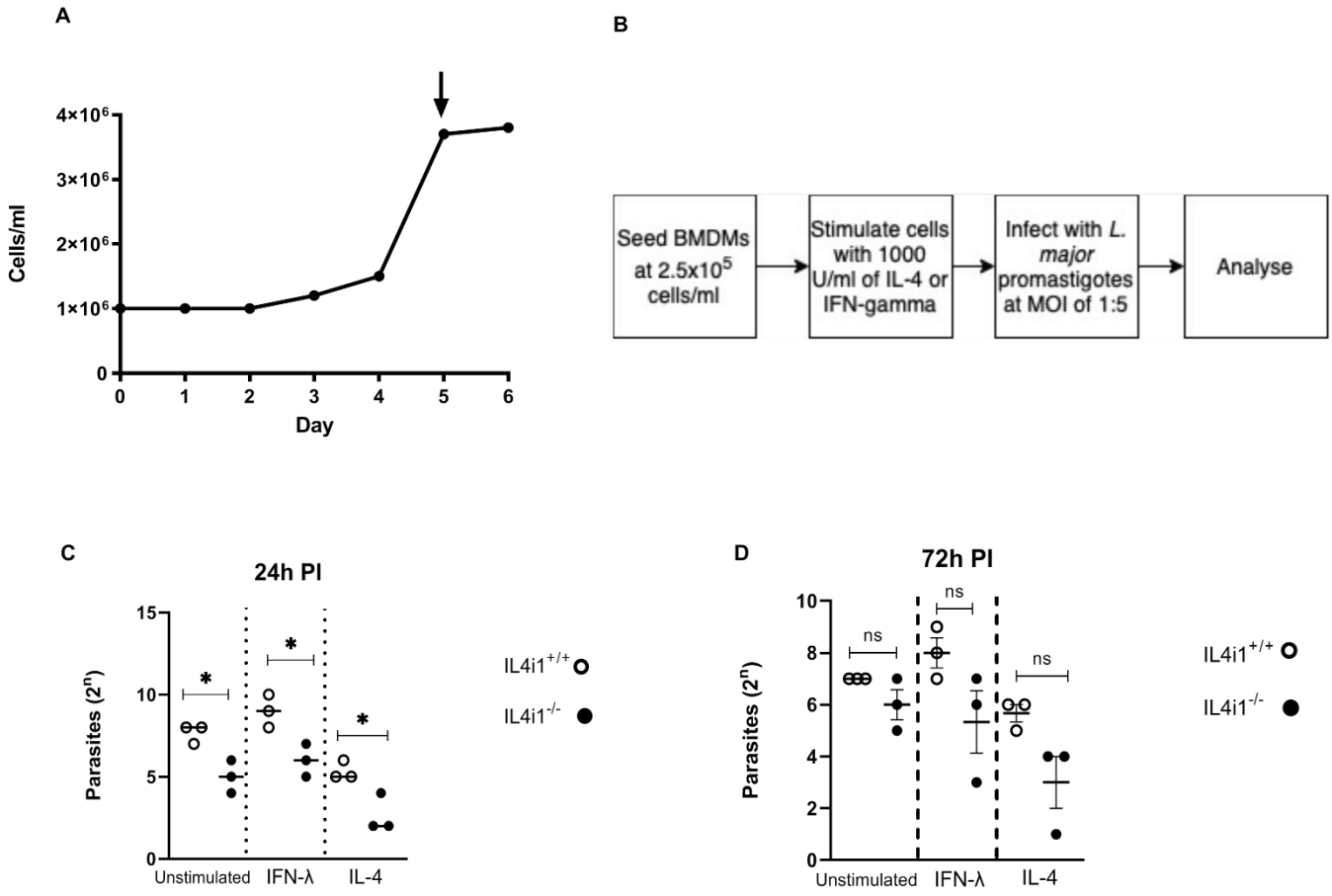

Figure 3.2. BMDMs infection with *L. major* promastigotes showing effect of parasite burden on stimulated BMDMs A) *L. major* promastigotes were seeded at 1x10^6 cells/ml media and counted every other day after being fixed with 4% paraformaldehyde exponential phase was reached**. B)** BMDMS were generated and 1x10^6 parasites were used to infected 2.5x10^5 BMDMs for both 24h and 72h after being stimulated with either IFN-***γ*** or IL-4 to mimic a Th1 or Th2 response, respectively. **C-D)** Parasite burden was quantified using a limiting dilution assay (LDA) at both 24h **(C)** and 72h **(D)** post-infection. Statistical analysis was performed using a non-parametric t-test defining difference to IL4i1$^{+/+}$ as significant. Data is representative of one independent experiment where n=3 for each group.

3.3 *IL-4i1*-deficient BMDMs show *L. major* infection role in disease progression by IL-10 production and inhibiting nitrite production

Since we found a decrease in parasite burden, cellular immune responses were analysed. Control of parasite replication is mediated by IFN-γ-derived IL-12 production by classically activated macrophages (Yue *et al*., 2015). Accordingly, cytokines (IL-10 and IL-12) and nitrite were analysed by sandwich enzyme-linked immunoabsorbent assay (ELISA) and the Griess assay respectively.

The production of nitrite is used as a proxy for iNOS activity in M1 macrophages (Ramona Hurdayal, 2017). **Figure 3.3 A** shows the concentration of nitrite produced by BMDMs from both IL-4i1$^{+/+}$ and IL-4i1$^{-/-}$ mice when stimulated by either IFN-γ or IL-4 at both 24 and 72h PI. At 24h (**Figure 3.3 A**), IL-4i1 $^{+/+}$ BMDMs infected with *L. major* and stimulated with IL-4 produced the highest amount of nitrite (30-40 μM) when compared to the IL-4i1$^{-/-}$ BMDMs that were also infected with *L. major* and stimulated with IL-4 (20 μM). While IL4i1$^{+/+}$ and IL4i1$^{-/-}$ IFN-γ-stimulated BMDMs infected with *L. major* produced the same levels of nitrite, overall, IL-4i1$^{-/-}$ BMDMs produced the highest amounts of nitrite when stimulated with IFN-γ. These data suggest that the absence of *IL4i1* could have a protective role against *leishmania major* infection.

Additionally, BMDMs were analysed via sandwich ELISA to detect the levels of IL-12 and IL-10 (Mohrs *et al*., 1999) secreted by macrophages (**Figures 3.3 B-E**). Levels of IL-12 detected at 24h PI (**Figure 3.3 B**) were similar across *L. major* infected IL-4i1$^{+/+}$ BMDMs stimulated with IL-4 when compared to those stimulated with IFN-γ. However, at 72h PI (**Figure 3.2 C**) IL-12 was not detected in IL-4i1$^{-/-}$ BMDMs infected with *L. major.* Additionally, IL-4i1$^{+/+}$ that were not infected produced and were stimulated with IL-4, produced the same amount of IL-12 as those stimulated with IFN-γ (4 ng/μl). Furthermore, at 72h PI (**Figure 3.3 C**) the levels of IL-12 produced by *L. major* infected IL-4i1$^{+/+}$ BMDMs stimulated with IFN-γ and IL-4 decreases as infection progresses. The same is shown in IL-4i1$^{-/-}$ BMDMs that have been infected and stimulated, with a noticeable difference of no

IL-12 being detected when compared to **Figure 3.3 B**. Taken together, **Figure 3.3 B** and **C** demonstrate that the absence of *IL-4i1* may have hampered M1 activation of BMDMs since IL-12 production was hindered. Additionally, IL-10 is an immunosuppressive cytokine which promotes M2 activation (Yue *et al*., 2015). Accordingly, levels of IL-10 were analysed at 24h and 72h PI (**Figure 3.3 D** and **E**). At 24h PI (**Figure 3.3 D**), the highest level of IL-10 was recorded at ± 10 ng/μl when IL-4i1$^{+/+}$ BMDMs were uninfected but stimulated with IFN-γ. This is interesting as IFN-γ is associated with M1 macrophage activation yet IL-10 production is associated with M2 macrophage activation (Hurdayal and Brombacher, 2017). Levels of IL-10 were mostly comparable between infected and IFN-γ and IL-4 treated BMDMs from IL-4i1$^{+/+}$ and IL-4i1$^{-/-}$. The highest levels of IL-10 were detected in 72hr PI in comparison to the 24hr IL-10 levels. 72hr PI was also distinguished by a different pattern. This pattern was specific to when IL4i1$^{-/-}$ BMDMs had been infected with *L. major* and stimulated with IFN-γ. However, after 72h the levels of IL-10 detected by IL-4i1$^{-/-}$ BMDMs infected with *L. major* increase from 5-10 ng/μl to 10 ng/μl. Taken together, the results shown in **Figure 3.3 D** and **E** indicate that the absence of *IL-4i1* in BMDMs increases IL-10 production, which is indicative of M2 macrophage activation (Hurdayal and Brombacher, 2017).

Collectively, the above results of *L. major* infected BMDMs demonstrate how the absence of *IL-4i1* effects disease progression a murine *in vitro* model. Next, was to analyse the role of *IL-4i1* in THP-1-derived macrophages as a proxy for a human *in vitro* model was investigated.

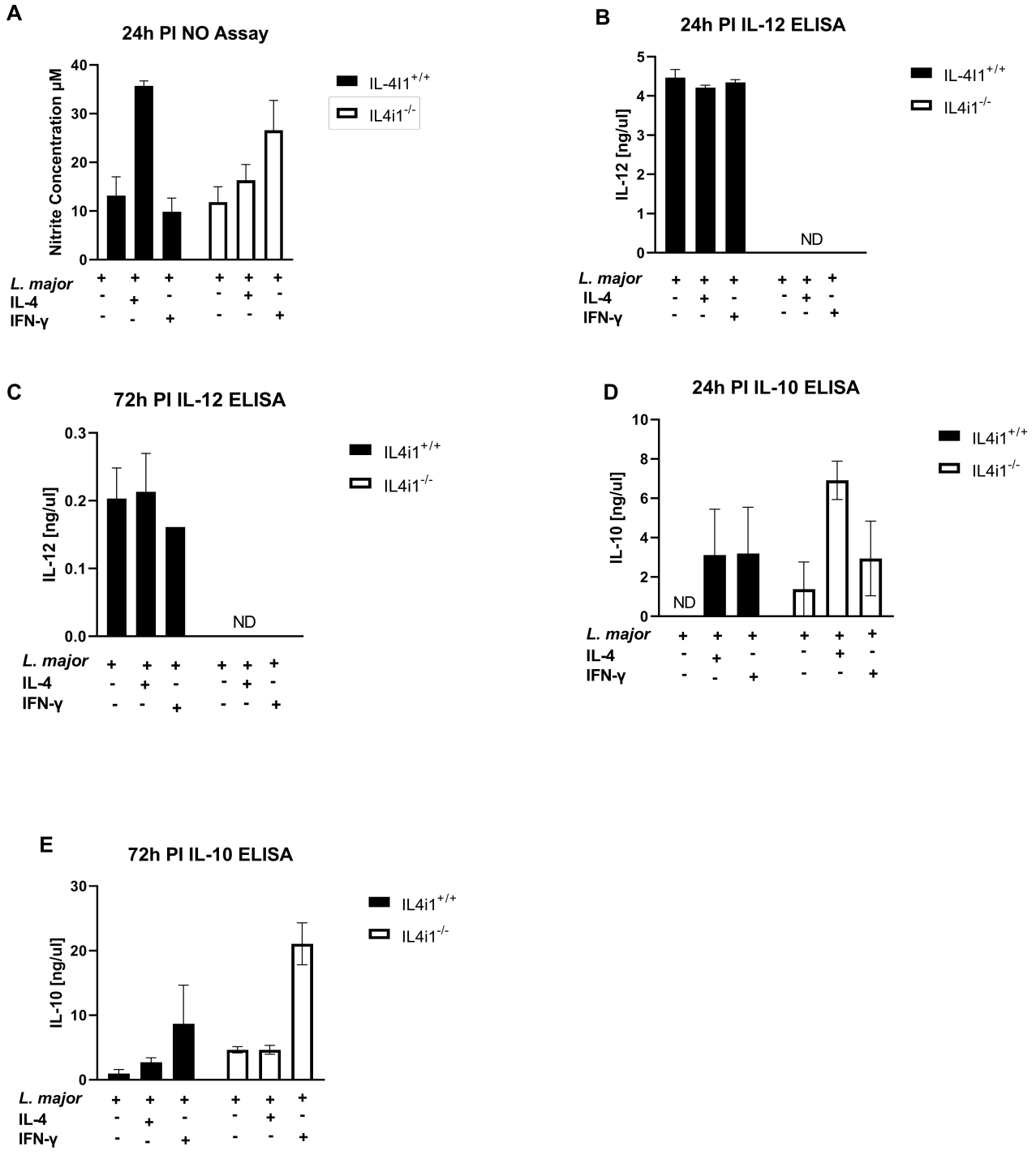

Figure 3.3 Bone-marrow derived macrophages infected with *L. major* promastigotes at MOI of 1:5 showing effects of *IL4i1* absence. **A)** Levels of nitrite produced by IL4i1$^{-/-}$ and IL4i1$^{+/+}$ BMDMs were detected at 24h post infection. **B-C)** An enzyme linked immunoabsorbent assay (ELISA) was used to detect the concentration of IL-12 at **B)** 24h and **C)** 72h post infection. **D-E)** Levels of IL-10 were detected using ELISAs at **D)** 24h and **E)** 72h post infection. Levels of IL-12, IL-10 and parasite burden were analyzed using a non-parametric t-test between IL4i1$^{-/-}$ and IL4i1$^{+/+}$ infected and uninfected samples. Data representative of one independent experiment where n=3 for each group. Data shown as +-SD with no statistical difference found (NS).

3.4 Generation of THP-1-derived macrophages from cultured THP-1 monocytes via phorbol 12-myristate 13-acetate (PMA)

THP-1 monocytes (strain number ATCC-TIB-202) were cultured in a humidified incubator and **Figure 3.3 A** depicts monocyte exponential growth in complete RPMI (10% FCS; 0.5% PenStrep; 0.1% Beta-mercaptoethanol). Confluency of the cells was measured by tryphan blue exclusion and was reached when cell count was $1x10^6$ cells/ml. Once THP-1 monocytes had been cultured successfully, they were differentiated into THP-1-derived macrophages using 20 ng/μl PMA. Differentiation was confirmed via flow cytometry where the forward and side scatters were analyzed. Forward and side scatter of macrophages show an increase in cell granularity and size (Forrester *et al*., 2018), which is indicative of successful differentiation from THP-1 monocytes to THP-1-derived macrophages **(Figure 3.3 B)**. Additionally, monocytes and macrophages were gated as per **Figure 3.4 C-E** for populations of $CD16^+$ and $CD14^+$. As per **Figure 3.4 E** monocyte populations are shown. Whereas **Figure 3.4 F-H** show the gating strategy for macrophages by checking for CD64 and CD16 positive populations. The shift of CD64 is the most important since monocyte-derived macrophages express CD64 more than monocytes (Aldo *et al*., 2013) hence the population shift as seen **in Figure 3.4 I** . Taken together, these results indicated the successful differentiation of THP-1 monocytes to THP-1-derived macrophages.

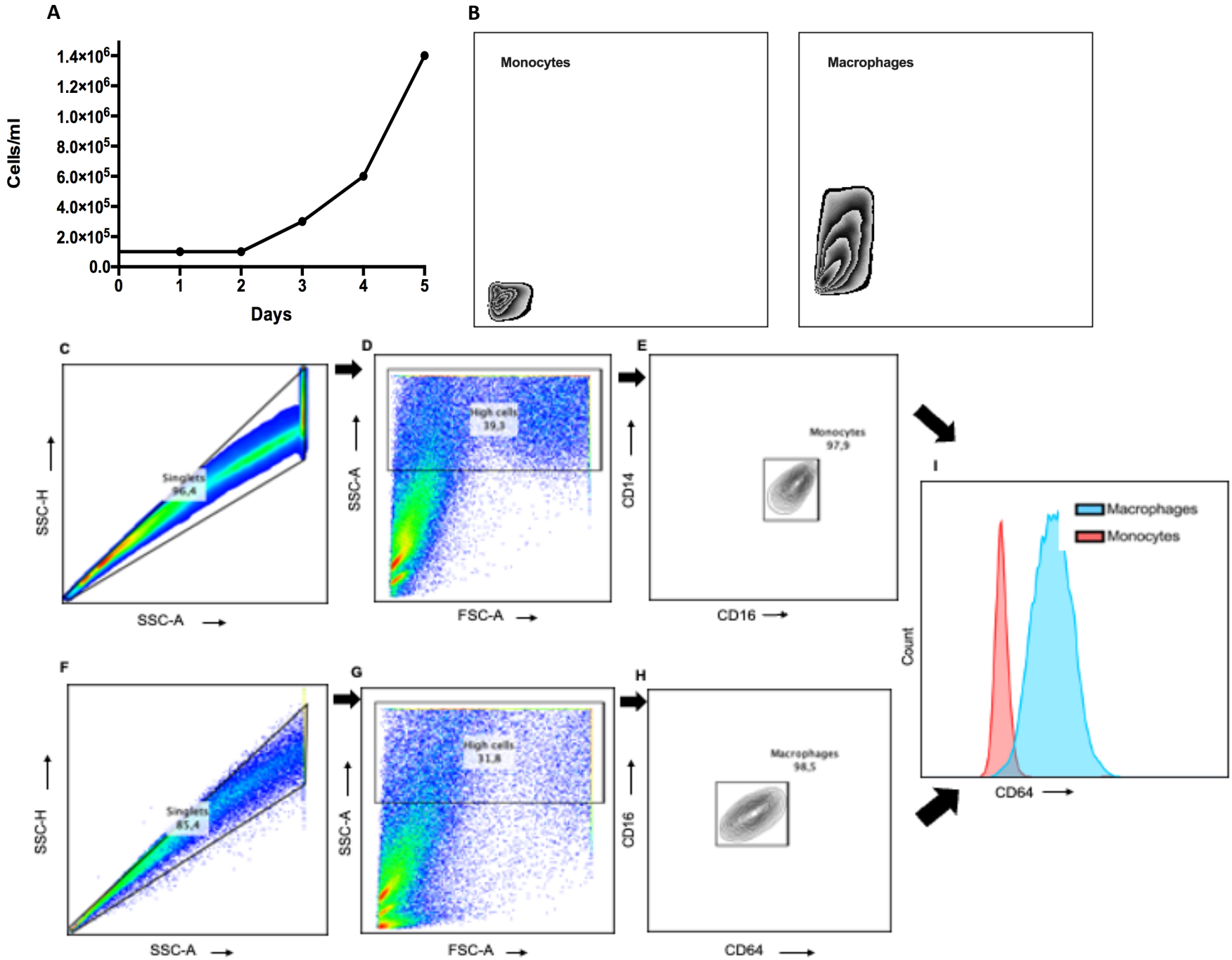

Figure 3.4. Generation of THP-1-derived macrophages from THP-1 monocytes using phorbol 12-myristate 13-acetate (PMA). A) Exponential growth of THP-1 monocytes monitored using trypan-blue exclusion. Confluency of $1x10^6$ cells/ml reached after five days in a humidified incubator at 37°C and 5% CO_2. **B)** forward and side scatters show an increase in macrophage cell granularity and size. **C-E)** Gating strategy for monocytes that are $CD14^+$ and $CD16^+$. **F-H)** Gating strategy for macrophages that are $CD64^+$ $CD16^+$. **I)** Histogram shift of $CD64^+$ populations before and after differentiation indicating THP-1-derived macrophages in blue and THP-1 monocytes in red.

3.5 *L. major* infection of THP-1-derived macrophages demonstrated higher parasite burden at 72h post-infection

Next, we infected THP-1-derived macrophages with *L. major* promastigotes to investigate infection kinetics and cell viability. Stationary phase *L. major* promastigotes (**Figure 3.2 A)** were used to infect $1x10^5$cells at MOI of 1:5 for 24 and 72 hours, respectively. Parasite burden was quantified by endpoint PCR using gene specific primers for kinetoplast DNA (kDNA). The size of kDNA is 120bp, (Ivens *et al*., 2005) and is specific to *Leishmania*, which amplified internalized amastigote parasites. **Figures 3.5 A** and **B** complement each other as the relative kDNA expression is semi-quantified by comparing band intensities of samples to a pure *L. major* isolated culture control using Image J software. Infection peaked at 24h and appeared reduced by 72h (**Figure 3.5 A**). To confirm that the infection reduction at 72h it was not due to cell viability being compromised, we performed an LDA. Accordingly, the LDA supplemented endpoint PCR data and investigated parasite burden of differentiated promastigotes. As shown in **Figure 3.5 C**, an increase in parasite burden at 72h PI was observed relative to 24h PI. Given that the changes in parasite burden could have been (**Figure 3.5 B**) due to host cell apoptosis and not due to the infection kinetic itself, we sought to test macrophage viability during infection. To determine this, a 3-(4,5-dimethylthiazol-2-yl)-2,5-diphenyl tetrazolium bromide (MTT) test was performed on infected samples to confirm macrophage viability. The principle of the MTT assay is based on a colourimetric change of a yellow dye to blue formazan products, which is only possible if cells are viable. **Figure 3.5 D** shows the exponential growth of THP-derived macrophages as the infection progressed. This demonstrated that no THP-1-derived macrophages were dead, and they continued to proliferate up to 6 days post-infection. Thus, indicated that parasite burden increased due to proliferation of THP-1-derived macrophages **(Figure 3.5 C)**.

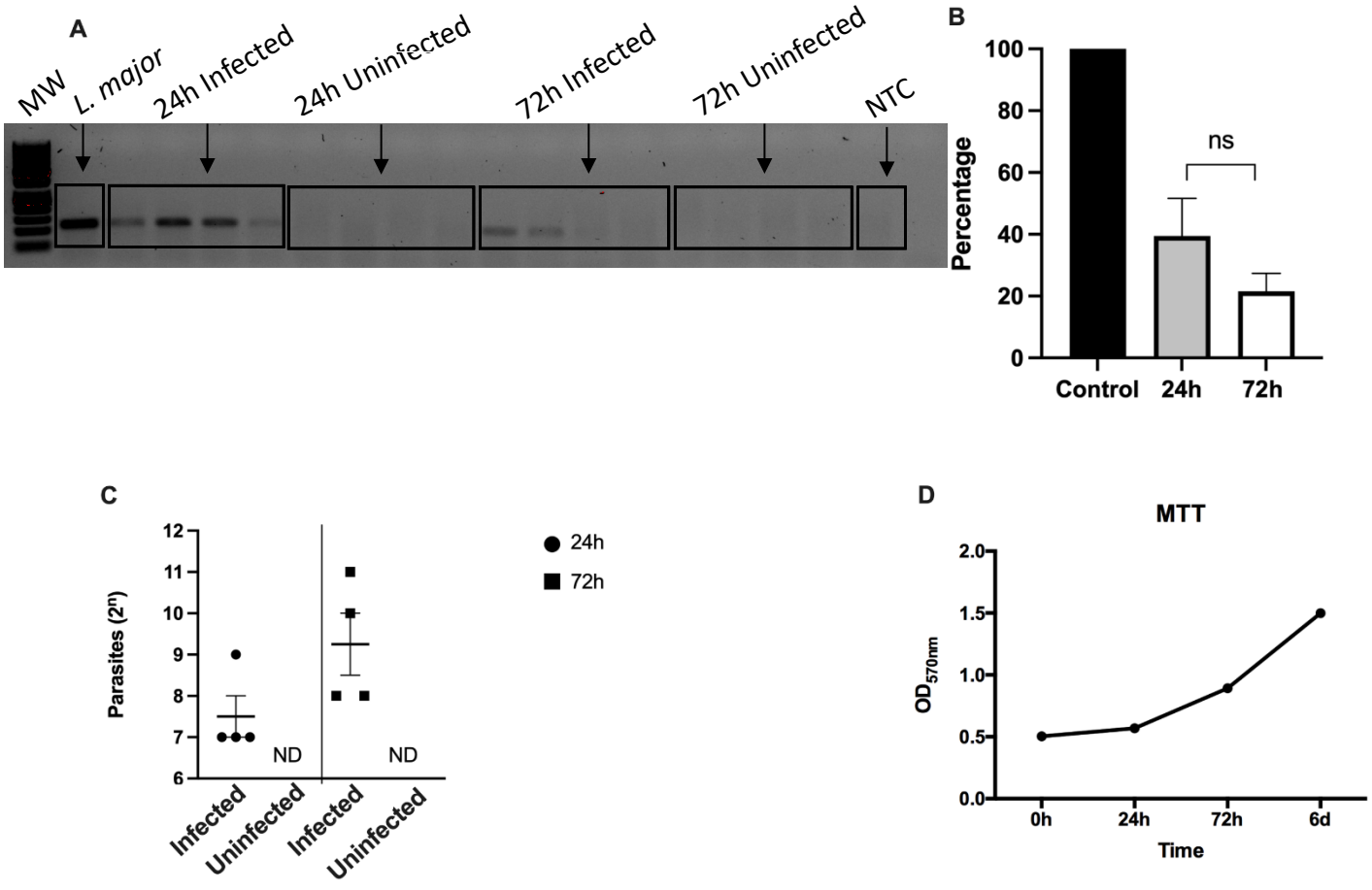

Figure 3.5. Infection of THP-1-derived macrophages with 1x10^6 *L. major* promastigotes. *L. major* promastigotes were seeded as per Figure 2A. **A)** Endpoint PCR of kDNA amplification from THP-derived macrophages at 24h and 72h PI for infected and uninfected samples. N=3 for each time point. **B)** Image J analysis of amplified kDNA using densitometry where relative expression was normalized to *L. major* cultured *in vitro.* **C)** Parasite burden assessed after 24, 72 hours via LDA where ND means not detected. Values shown are calculated from n=4 for both infected and uninfected cells and shown as SEM. Significance calculated as comparing uninfected with infected at each time point. P<0.0001 shown as ****. **D)** Viability of infected THP-derived macrophages detected via absorbance values of formazan product formed in live cells. Non-parametric t-test was used to calculate significance in LDA and kDNA expression where no significance was apparent. Data is representative of one independent experiment. Data is shown as +-SD.

3.6 Gene-silencing of *GAPDH* in THP-1-derived macrophages using *GAPDH* specific siRNA Select Silencers™ and Lipofectamine 3000™

We next sought to confirm that THP-1-derived macrophages could be silenced using the siRNA Select Silencers™ and Lipofectamine 3000™, as a platform for silencing *IL-4i1* in THP-1-derived macrophages. Firstly, we compared the use of two different silencing medias, the main difference being the absence of sera as it has been known to inhibit lipofectamine (**Figures 3.6 A** and **B**) (Mo *et al.*, 2012). The first media contained 1% PenStrep and no FCS in RPMI-1640. As shown in **Figure 3.6 A** ,this media equated to 20% knock down efficiency (KD) indicating that 80% of *GAPDH* gene expression remained (RE). This was evaluated using the $2^{-\Delta\Delta Ct}$ method with *18S* being the housekeeping gene and *GAPDH* used as the internal positive control. The second media contained only RPMI-1640 media and showed a 100% KD efficiency. Therefore, this indicated that antibiotics and sera may have had an inhibitory effect on the transfection agent Lipofectamine 3000™. Furthermore, **Figure 3.6 C** shows the significant genetic expression decrease of *GAPDH* compared to *18S.* Together, these figures demonstrate that Lipofectamine 3000™ and siRNA Select Silencers™ yielded more than 80% knockdown efficiency of *GAPDH* when used on THP-1-derived macrophages that are between 50-60% confluent at the time of transfection.

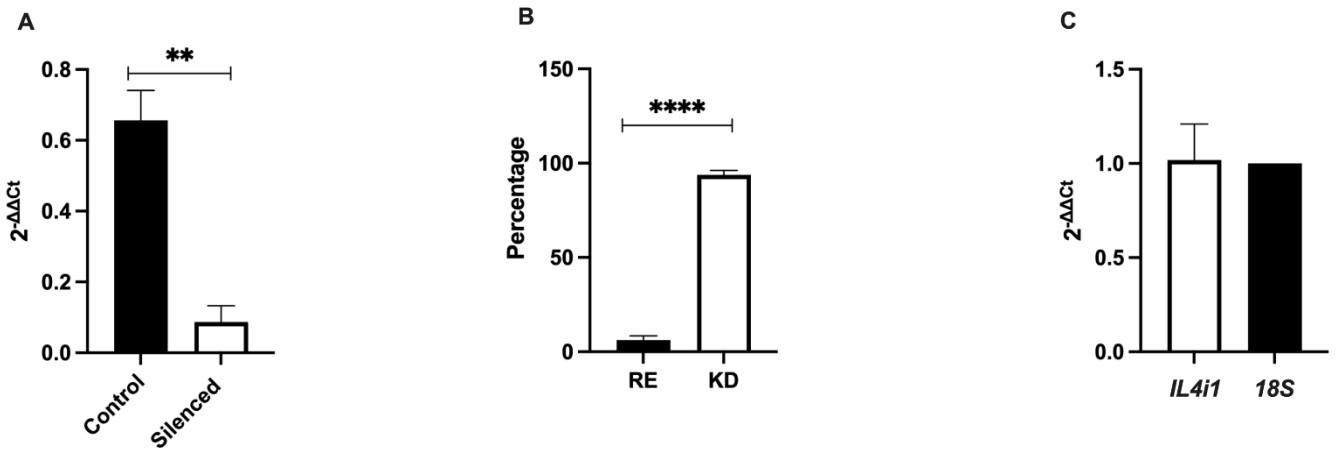

Figure 3.6. *GAPDH* silencing in THP-1-derived macrophages using *18S* as the housekeeping gene where expression was measured using the $2^{-\Delta\Delta Ct}$ method. A) 20% knockdown of *GAPDH* achieved when using first media (RPMI-1640; 1% Penstrep). **B)** 100% knockdown of *GAPDH* when using second media (RPMI-1640) **C)** Relative expression of *GAPDH* as compared to *18S* as the housekeeping gene. The $2^{-\Delta\Delta Ct}$ method was used. Statistical significance was calculated using a non-parametric t-test between RE and KD. Data representative of 3 independent experiments where n=3 for each group. P<0.05 shown as * and p<0.001 shown as ****.

3.7 Gene-silencing of *IL4i1* in THP-1-derived macrophages using *IL4i1* specific siRNA Select Silencers™ and Lipofectamine 3000™

We used the experimental setup as in **Figure 3.6** to perform gene-specific silencing of *IL4i1* in THP-1-derived macrophages using siRNA Select Silencers™. Using the same silencing media as in **Figure 3.6 B** which was only RPMI-1640, **Figures 3.7 A** and **B** show that silencing of *IL4i1* was successfully achieved. Relative gene expression between *IL4i1* and *18S* (reference gene) shown in **Figure 3.7 A** indicate the difference in genetic expression of *IL4i1* that has been silenced which is about 3x less than *18S* expression. This is further reinforced in **Figure 3.7 B** as the remaining gene expression (RE) percentage is almost 10% and knockdown efficiency (KD) is at 90%. Notably, **Figure 3.7 C** showed the normal gene expression of *IL4i1* without being exposed to any stimuli to accurately show decrease in expression of *IL4i1* due to the absence of *IL-4i1* expression.

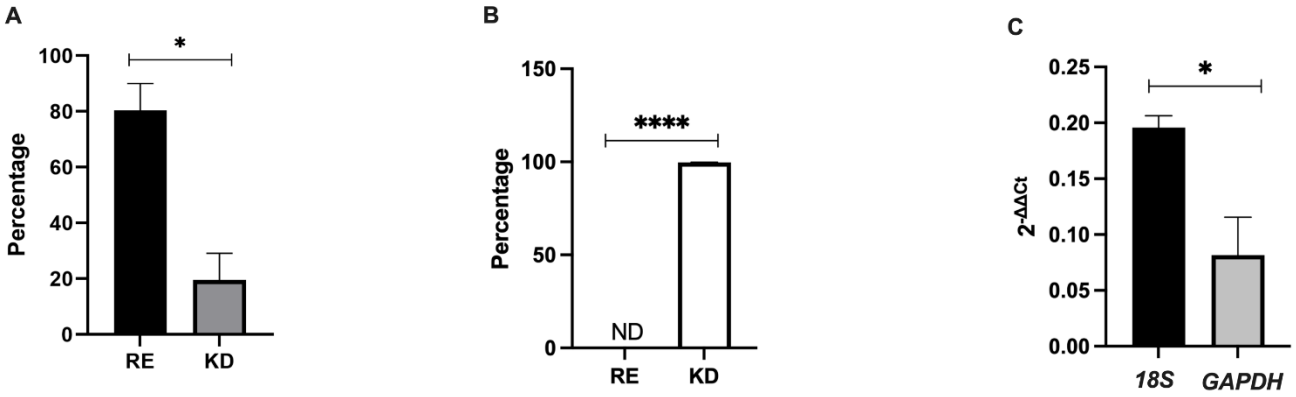

Figure 3.7. Gene-silencing of *IL4i1* in THP-1-derived macrophages using *18S* as the housekeeping gene where expression was measured using the $2^{-\Delta\Delta Ct}$ method. A) Expression of *IL4i1* in THP-1-derived macrophages seeded at $4x10^4$ cells/100μl in RPMI-1640 compared to *18S* as the housekeeping gene using the $2^{-\Delta\Delta Ct}$ method. **B)** Expression of *IL4i1* gene-silencing shown as remaining gene expression (RE) at almost 10% and knock down (KD) efficiency at 90%. **C)** Normal *IL4i1* gene expression in THP-1-derived macrophages. Data are representative of 3 independent experiments where n=3 for each group. Statistical significance was calculated using non-parametric t-test where ** is $p<0.001$ and *** is $p<0.0001$.

3.8 *L. major* infection studied in *IL4i1* silenced THP-1-derived macrophages

We next sought to investigate response to *L. major* infection in *IL4i1* silenced-THP-1-derived macrophages . Firstly, we analysed efficiency of knockdown post *L. major* infection. After a qPCR was done, **Figure 3.8 A** shows that gene-silencing of *IL4i1* is maintained 24h post infection. Since *IL4i1* silencing occurred 24h prior to infection, silencing of *IL4i1* was maintained 48h post transfection with almost 100% knock down efficiency as calculated using the $2^{-\Delta\Delta Ct}$ method **(Figure 3.8 A)**. *18S* was used as housekeeping control in **Figure 3.8 B** and similarly to **Figure 3.7 A**, *IL4i1* expression appears to be at least 3x less than *18S.* Notably, *L. major* infection had no effect on *IL4i1* silencing as infected and uninfected *IL4i1* silenced THP-1-derived macrophages was not significant. IL-4i1 could regulate infection by promoting or suppressing CL progression. We therefore analysed parasite burden in silenced and unsilenced THP-1-derived macrophages following

infection. Analysis revealed that presence of IL-4i1 promoted parasite replication as at 24h PI, parasite burden in *IL-4i1 silenced*- THP-1-derived macrophages was significantly lower than infected THP-1-deroved macrophages with normal IL-4i1 expression. Notably those that were just infected with *L. major* had a higher burden than silenced THP-1-derived macrophages that were also infected with *L. major*. However, at 72h PI (**Figure 3.8 D**), burden for both was the same with a doubled burden for silenced THP-1-derived macrophages and their infected counterparts.

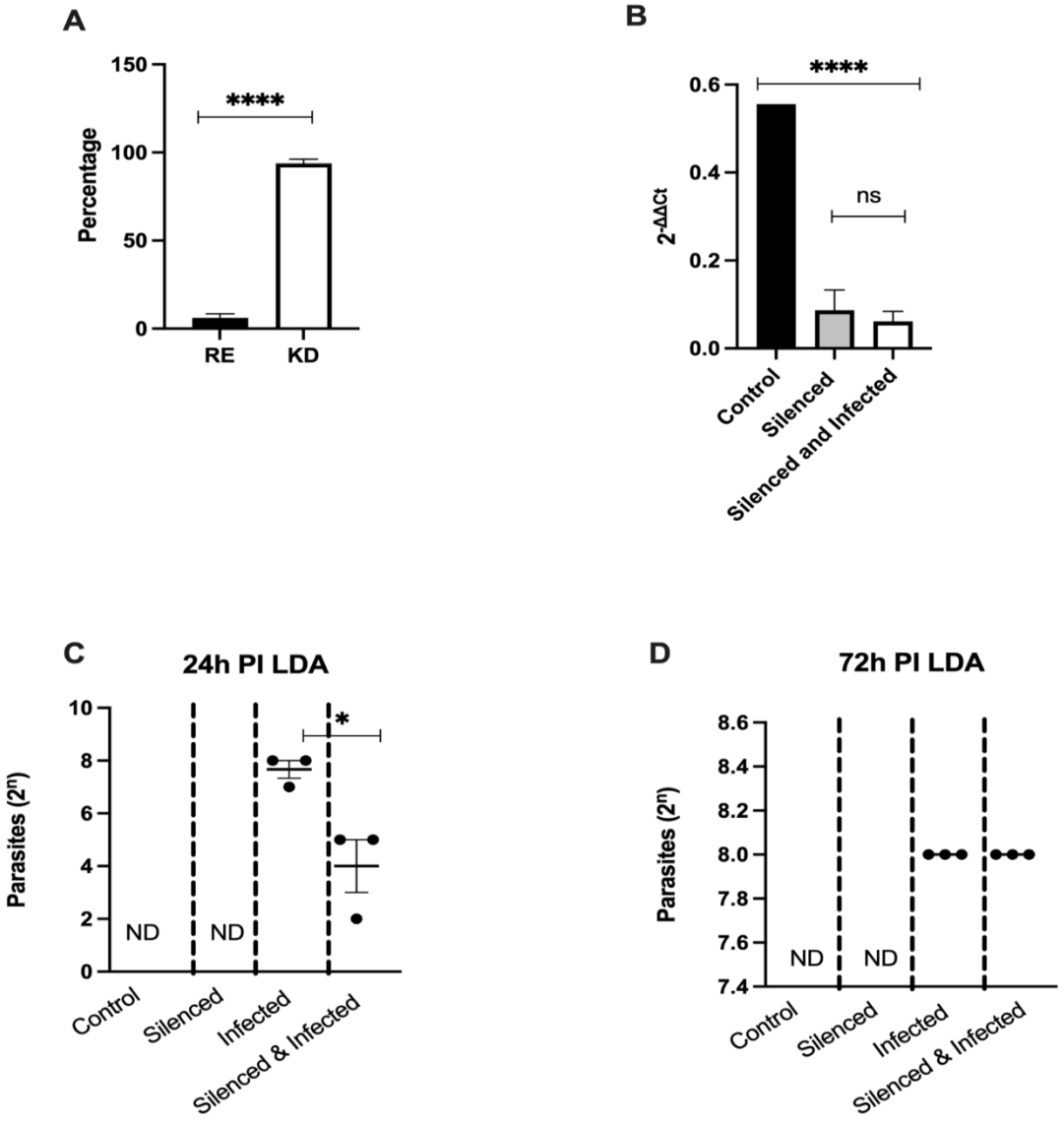

Figure 3.8. Infecting THP-1-derived macrophages with *L. major* promastigotes at MOI of 1:5 shows the difference between silenced and normal *IL4i1* gene expression. Parasites were seeded as Figure 3.2 A and THP-1-derived macrophages were seeded at $2x10^5$ cells/ml and infected

at an MOI of 1:5. **A)** *IL4i1* gene-silencing is maintained when THP-1-derived macrophages are infected shown as remaining gene expression (RE) and gene knock down (KD). **B)** No statistical significance between silenced and silenced and infected THP-1-derived macrophages. **C-D)** Parasite burden was quantified using a limiting dilutions assay (LDA) and concentrations were recorded at both **C)** 24h and **D)** 72h post infection. Statistical significance was calculated using a non-parametric t-test. Significance ($p>0.001$) is shown as ****. Data are representative of two independent experiments where n=3 for each group. Data is shown as +- SD.

3.9 Gene-silencing of *IL4i1* in THP-1-derived macrophages shows a non-protective role of *IL4i1* against *L. major* infection

Following analysis of parasite burden, cellular immune responses were analysed in *IL-4i1* silenced THP-1-derived macrophages following *L. major* infection. Arginase and iNOS are important in leishmania infection because they allow for parasite proliferation. Accordingly, levels of nitrite, as a proxy for NO production and M1 activation, was analysed. At 24h PI (**Figure 3.9 A**) silenced and infected THP-1-derived macrophages produced the highest levels of nitrite (0.4 μM) when compared to THP-1-derived macrophages that were solely infected or silenced. However, **Figure 3.9 B** (72h PI) showed the decrease of these levels at least 10x to 0.04μM. Indicating that after 72h of *L. major* infection, the absence of *IL-4i1* did not protect against disease progression but rather steered macrophages towards an M2 activation.

Additionally, sandwich ELISAs were conducted for the detection of IL-12. IL-12 is a cytokine associated with M1 macrophage activation and can give insight to macrophage polarization of silenced and infected THP-1-derived macrophages (Aruleba *et al*., 2020). At 24h PI, silenced and infected THP-1-derived produced the lowest amount of IL-12 when compared to THP-1-derived macrophages that were solely infected or silenced. However, THP-1-derived macrophages that were either infected or silenced produced similar amount of IL-12 to each other; but when combined, the gene-silencing of *IL-4i1* and infection with *L. major* negated each other. This indicated that THP-1-derived macrophages were steered towards M2 activation.

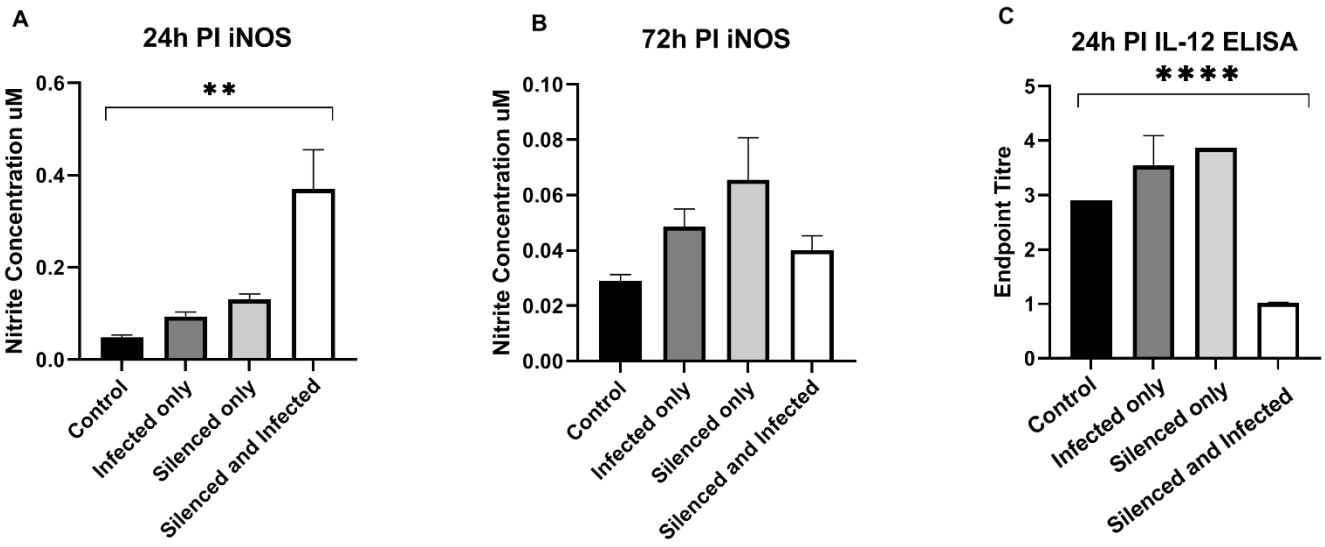

Figure 3.9. THP-1-derived macrophages infected with *L. major* promastigotes at MOI of 1:5 showing effects of gene-silencing of *IL4i1*. Parasites were seeded as Figure 2A while THP-1 cells were prepared as Figure 3B. THP-1-derived macrophages were seeded at $2x10^5$ cells/ml and infected at an MOI of 1:5. **A-B)** Concentration of nitrite oxide (NO) produced by $IL4i1^{-/-}$ and $IL4i1^{+/+}$ THP-1-derived macrophages was measured at **A)** 24h and **B)** 72h. An enzyme linked immunoabsorbent assay (ELISA) was used to detect the levels of **C)** IL-12 at 24h PI. Levels of IL-12 was analyzed using a non-parametric t-test between control, infected, silenced, and silenced and infected THP-1-derived macrophages, except a one-way ANOVA was used for calculating significance of nitrite concentration where ** is $p<0.005$. Data representative of one independent experiment where n=3 for each group. Data is shown as +- SD.

4. Discussion and conclusion

The aim of this study was to characterize the role of IL-4i1 as a host immunoregulator in cell-based systems when infected with *L. major* (cutaneous leishmaniasis). This aim was achieved by using *IL-4i1*-deficient BALB/c mice to generate bone-marrow derived macrophages (BMDMs) as well as using Silencer Select siRNAs™ to silence *IL-4i1* in THP-1-derived macrophages. After infecting both cell lines with *L. major*, IL-4i1's role was characterized by assessing the infection kinetics in the absence of *IL-4i1.* This was evaluated by quantifying parasite burden and the amount of nitrite that was produced 24h and 72h post-infection in both BMDMs and THP-1-derived macrophages. Increased parasite burden was found in *L.* major infected THP-1-derived macrophages suggesting that the presence of *IL-4i1* causes disease susceptibility. However, upon silencing *IL-4i1,* parasite burden decreased, implying that the absence of *IL-4i1* offers protection against disease. This same pattern was observed in parasite burden of BMDMs, where the absence of *IL-4i1* offered disease protection.

The use of *in vitro* models has shown how *Leishmania* parasites have been evading attacks by the host immune system. The first 24-72 hours are crucial for infection kinetics. During this period, the host system will decide between activating the Type 1 or 2 response, where either protection or susceptibility will be established, respectively (Hurdayal and Brombacher, 2017). As illustrated in Figure 1.1, when IL-4 has been secreted by myeloid lineage cells, alternative (M2) activation of macrophages is stimulated. This ultimately leads to a type 2 immune response, which favours the progression of CL. The opposite is true when cells have been stimulated with IFN-γ, classical activation (M1) of macrophages is produced, resulting in the destruction of parasites (Govender *et al*., 2018) Sacks and Kamhawi, 2001). Given that murine cell lines, like BMDMs could be stimulated with both IFN-γ and IL-4, the effect of polarization on the outcome of *L. major* infected macrophages also examined in this study.

It has been shown that disease outcome can be influenced by macrophage polarization (Sacks and Kamhawi, 2001). This is primarily the result of Th1 or Th2 immune responses, which will protect against or allow disease progression, respectively (Cousin *et al*., 2015). Cytokines like IL-12 and IL-10 will be secreted by BMDMs or THP-1-derived macrophage as an indication of M1 or M2 macrophage activation, respectively (Mills, 2015). IL-10 was not detected at either 24h or 72h PI in silenced-THP-1-derived macrophages. This could result from cell apoptosis that could not survive the strain of gene-silencing and infection with *L. major* (Genin *et al*., 2015). This could also be the result of few cells being infected as an MOI of 5 could also be strenuous on cells, causing cell death (Getti *et al*., 2008).

Another important finding is the amount of nitrite that both BMDMs and THP-1-derived macrophages produced. The production of nitrite is used as a proxy to determine the level of inducible nitric oxide synthase (iNOS) activity (Hurdayal and Brombacher, 2017). The production of nitrite is indicative of M1 macrophage activation, i.e., nitrite will be produced if cells like macrophages have been stimulated with IFN-γ (Kopf et al., 1996). At 24h PI of IL-4i1$^{+/+}$ BMDM, the highest level of nitrite was detected when stimulated with IL-4, which could indicate that even though the BMDMs have been alternatively (M2) activated, the presence of nitrite indicates that the cells are fighting disease progression. Taken together, this implies that the absence of *IL-4i1* has a protective role on BMDMs since the production of nitrite is associated with M1 activation and ultimately type 1 immune response (Figure 1.1) where the opposite has been reported (Yue *et al*., 2015).

Additionally, nitrite has a killing effect on *L. major* parasites (Ribeiro *et al*., 2020). By measuring the parasite burden of both BMDMs and THP-1-derived macrophages, we could relate the results to nitrite production to find any trends. At 24h PI, parasite burden was lowest in IL-4i1$^{-/-}$ BMDMs that were stimulated with IL-4, which correlates to the least amount of nitrite produced, allowing parasites to proliferate. This demonstrates that the presence of *IL-4i1* causes susceptibility in

BMDMs. Since nitrite was not detected at 72h PI of BMDMS, it can only be implied that due to less parasite burden there should have been more nitrite produced (Ribeiro *et al*., 2020). Comparably, parasite burden in silenced THP-1-derived macrophages after 24h of infection with *L. major* was the least. This result correlates with the highest levels nitrite that have been produced, indicative of parasite killing. These findings are opposite to those seen in Yue *et al*., (2015), where the presence of *IL4-i1* promoted M2 macrophage activation.

Moreover, when nitrite production by BMDMs was compared to THP-1-derived macrophages more nitrite was produced by BMDMs than by THP-1-derived macrophages. This could imply M1 activation of macrophages, indicating that the presence of *IL-4i1* makes THP-1-derived macrophages more susceptible to *L. major*. Contrastingly, at 72h PI the overall amount of nitrite produced decreases and infected and silenced THP-1-derived macrophages produced less nitrite as infection progressed further implying the dichotomy of *IL-4i1* (Cousin *et al*., 2015; Molinier-Frenkel *et al*., 2019).

The role of *IL-4i1* in host immunity is attractive in leishmaniasis due to its dichotomy as seen above. It has been shown that IL-4i1 affects T effector and memory cells that could be detrimental to cell proliferation, thus allowing disease progression (Cousin *et al*., 2015). Contrastingly, IL-4i1 alters the cells microenvironment by producing hydrogen peroxide and catabolizing phenylalanine, ultimately starving, and killing *Leishmania* parasites (Molinier-Frenkel *et al*., 2019). By measuring the amount of hydrogen peroxide produced, other studies have identified it as having major killer effector functions (Kasai *et al*., 2005). This study could further investigate this as a supplementary result to nitrite production and its effect on parasite burden. During the catabolism of phenylalanine, water, and oxygen by IL-4i1, hydrogen peroxide is not the only byproduct as phenylpyruvate, and ammonia are also released (Figure 3). Ammonia alters the pH of the cell's microenvironment and phenylalanine is an amino acid that *Leishmania* parasites cannot create themselves, hence IL-4i1 depletes this substrate and starves the parasites

(Grohmann and Bronte, 2010). These factors make IL-4i1 a potential target for host-directed therapies as it does not affect the *Leishmania* parasites but rather enhances the host immune response to leishmaniasis (Aruleba *et al*., 2020).

In the future, we would like to explore other targets for HDTs like cysteinyl leukotriene receptors (CystLR). Other studies have shown that using THP-1-derived macrophages are beneficial for leishmaniasis research (Esfandiari *et al*., 2019) (dos Santos *et al*., 2017) (Souza *et al*., 2021). With the shortest doubling time compared to cell lines like U-937 and Mono Mac 6 (Table 2) they are most favoured. Furthermore, murine cell lines like BMDMs have also been used in the leishmanial context extensively (Modolell *et al*., 1995) (Yue *et al*., 2015). Both cell lines can be gene-silenced for either CystLR (1 or 2), revealing how *Leishmania* parasites gain entry to target cells and could thus be a potential target for HDTs (Serezani *et al*., 2006). Importantly, data gathered from this study lacks power as the sample numbers were small. While, increasing sample sizes and number of repeats was planned, time and cost restraints prevented this.

Additionally, future research can use different strains of leishmaniasis. This study focused on *L. major* which causes cutaneous leishmaniasis, but other studies have used *L. braziliensis* to study mucocutaneous leishmaniasis or *L. donovani* to study visceral leishmaniasis (Donovan *et al*., 2012) (Souza *et al*., 2021) in the context of THP-1-derived macrophages. Furthermore, the lack of an effect at 72 hours could indicate IL-4i1 plays a role in the ability of *L. major* to establish infection in macrophages and that once the infection is established, any effect on the host is mediated through the mediators the infected macrophages release albeit after initiation of infections has been affected. Indeed, this could be investigated by washing the free parasites after 24h infection to examine the effect of 72h infection with the phagocyted parasites.

In conclusion, this study has provided information on gene-silencing of *IL-4i1* in both a murine and human cell model during infection with CL. The gene-silencing

of *IL-4i1* has shown contrasting roles in human and murine models, with both models showing that its presence causes susceptibility at different times during infection with *L. major.* Since most treatments and drugs target the parasites themselves, there has been a need for new approaches since parasites gain resistance against drugs over time. A popular idea is to explore candidates for host-directed therapies. Considering this, this study focused on determining whether *IL4i1* could be a target for such therapies due to its role in the immune response to different cell hosts.

5. References

ALDO, P. B., CRAVEIRO, V., GULLER, S. & MOR, G. 2013. Effect of culture conditions on the phenotype of THP-1 monocyte cell line. *Am J Reprod Immunol,* 70**,** 80-6.

ALJANABI, S. M. & MARTINEZ, I. 1997. Universal and rapid salt-extraction of high quality genomic DNA for PCR-based techniques. *Nucleic acids research,* 25**,** 4692-4693.

ANYANWU, S. I., DOHERTY, A., POWELL, M. D., OBIALO, C., HUANG, M. B., QUARSHIE, A., MITCHELL, C., BASHIR, K. & NEWMAN, G. W. 2018. Detection of HIV-1 and human proteins in urinary extracellular vesicles from HIV+ patients. *Advances in virology,* 2018.

ARULEBA, R. T., CARTER, K. C., BROMBACHER, F. & HURDAYAL, R. 2020. Can We Harness Immune Responses to Improve Drug Treatment in Leishmaniasis? *Microorganisms,* 8.

BANKOTI, R. & STÄGER, S. 2012. Differential regulation of the immune response in the spleen and liver of mice infected with Leishmania donovani. *Journal of tropical medicine,* 2012.

BURZA, S., CROFT, S. L. & BOELAERT, M. 2018. Leishmaniasis. *The Lancet,* 392**,** 951-970.

CDC. 2020. *Leishmaniasis* [Online]. https://www.cdc.gov/parasites/leishmaniasis/biology.html. Available:

https://www.cdc.gov/parasites/leishmaniasis/biology.html [Accessed 10 October 2020].

CHANPUT, W., MES, J. J. & WICHERS, H. J. 2014. THP-1 cell line: An in vitro cell model for immune modulation approach. *International Immunopharmacology,* 23**,** 37-45.

CHOI, C. M. & LERNER, E. A. 2001. Leishmaniasis as an Emerging Infection. *Journal of Investigative Dermatology Symposium Proceedings,* 6**,** 175-182.

COUSIN, C., AUBATIN, A., LE GOUVELLO, S., APETOH, L., CASTELLANO, F. & MOLINIER-FRENKEL, V. 2015. The immunosuppressive enzyme IL4I1 promotes FoxP3+ regulatory T lymphocyte differentiation. *European journal of immunology,* 45**,** 1772-1782.

DAS, M., MUKHERJEE, S. B. & SHAHA, C. 2001. Hydrogen peroxide induces apoptosis-like death in Leishmania donovani promastigotes. *Journal of Cell Science,* 114**,** 2461-2469.

DAYAKAR, A., CHANDRASEKARAN, S., KUCHIPUDI, S. V. & KALANGI, S. K. 2019. Cytokines: key determinants of resistance or disease progression in visceral leishmaniasis: opportunities for novel diagnostics and immunotherapy. *Frontiers in immunology***,** 670.

DE MATTOS ALMEIDA, M. C., CAIAFFA, W. T., ASSUNÇÃO, R. M. & PROIETTI, F. A. 2007. Spatial Vulnerability to Dengue in a Brazilian Urban Area During a 7-Year Surveillance. *Journal of Urban Health,* 84**,** 334-345.

DESCLOUX, E., MANGEAS, M., MENKES, C. E., LENGAIGNE, M., LEROY, A., TEHEI, T., GUILLAUMOT, L., TEURLAI, M., GOURINAT, A.-C., BENZLER, J., PFANNSTIEL, A., GRANGEON, J.-P., DEGALLIER, N. & DE LAMBALLERIE, X. 2012. Climate-Based Models for Understanding and Forecasting Dengue Epidemics. *PLOS Neglected Tropical Diseases,* 6**,** e1470.

DONOVAN, M. J., TRIPATHI, V., FAVILA, M. A., GERACI, N. S., LANGE, M. C., BALLHORN, W. & MCDOWELL, M. A. 2012. Indoleamine 2,3-dioxygenase (IDO) induced by Leishmania infection of human dendritic cells. *Parasite Immunology,* 34**,** 464-472.

DOS SANTOS, J. C., HEINHUIS, B., GOMES, R. S., DAMEN, M. S. M. A., REAL, F., MORTARA, R. A., KEATING, S. T., DINARELLO, C. A., JOOSTEN, L. A. B. & RIBEIRO-DIAS, F. 2017. Cytokines and microbicidal molecules regulated by IL-32 in THP-1-derived human macrophages infected with New World Leishmania species. *PLOS Neglected Tropical Diseases,* 11**,** e0005413.

DUQUE-BENÍTEZ, S. M., RÍOS-VÁSQUEZ, L. A., OCAMPO-CARDONA, R., CEDEÑO, D. L., JONES, M. A., VÉLEZ, I. D. & ROBLEDO, S. M. 2016. Synthesis of novel quaternary ammonium salts and their in vitro antileishmanial activity and U-937 cell cytotoxicity. *Molecules,* 21**,** 381.

EGUI, A., LEDESMA, D., PÉREZ-ANTÓN, E., MONTOYA, A., GÓMEZ, I., ROBLEDO, S. M., INFANTE, J. J., VÉLEZ, I. D., LÓPEZ, M. C. & THOMAS, M. C. 2018. Phenotypic and functional profiles of antigen-specific CD4+ and CD8+ T cells associated with infection control in patients with cutaneous leishmaniasis. *Frontiers in cellular and infection microbiology***,** 393.

ENGELS, D. & ZHOU, X.-N. 2020. Neglected tropical diseases: an effective global response to local poverty-related disease priorities. *Infectious Diseases of Poverty,* 9**,** 10.

ESFANDIARI, F., MOTAZEDIAN, M. H., ASGARI, Q., MOROWVAT, M. H., MOLAEI, M. & HELI, H. 2019. Paromomycin-loaded mannosylated chitosan nanoparticles: Synthesis, characterization and targeted drug delivery against leishmaniasis. *Acta Tropica,* 197**,** 105072.

FENOLLAR, F. & MEDIANNIKOV, O. 2018. Emerging infectious diseases in Africa in the 21st century. *New Microbes and New Infections,* 26**,** S10-S18.

FORRESTER, M. A., WASSALL, H. J., HALL, L. S., CAO, H., WILSON, H. M., BARKER, R. N. & VICKERS, M. A. 2018. Similarities and differences in surface receptor expression by THP-1 monocytes and differentiated macrophages polarized using seven different conditioning regimens. *Cellular Immunology,* 332**,** 58-76.

GENIN, M., CLEMENT, F., FATTACCIOLI, A., RAES, M. & MICHIELS, C. 2015. M1 and M2 macrophages derived from THP-1 cells differentially modulate the response of cancer cells to etoposide. *BMC cancer,* 15**,** 1-14.

GETTI, G., CHEKE, R. & HUMBER, D. 2008. Induction of apoptosis in host cells: A survival mechanism for Leishmania parasites? *Parasitology,* 135**,** 1391-9.

GOVENDER, M., HURDAYAL, R., MARTINEZ-SALAZAR, B., GQADA, K., PILLAY, S., GCANGA, L., PASSELLI, K., NIEUWENHUIZEN, N. E., TACCHINI-COTTIER, F., GULER, R. & BROMBACHER, F. 2018. Deletion of Interleukin-4 Receptor Alpha-Responsive Keratinocytes in BALB/c Mice Does Not Alter Susceptibility to Cutaneous Leishmaniasis. *Infection and Immunity,* 86**,** e00710-18.

GROHMANN, U. & BRONTE, V. 2010. Control of immune response by amino acid metabolism. *Immunological reviews,* 236**,** 243-264.

GULER, R., PARIHAR, S. P., SAVVI, S., LOGAN, E., SCHWEGMANN, A., ROY, S., NIEUWENHUIZEN, N. E., OZTURK, M., SCHMEIER, S., SUZUKI, H. & BROMBACHER, F. 2015. IL-4Rα-Dependent Alternative Activation of Macrophages Is Not Decisive for Mycobacterium tuberculosis Pathology and Bacterial Burden in Mice. *PLOS ONE,* 10**,** e0121070.

GUZMAN, A. & ISTÚRIZ, R. E. 2010. Update on the global spread of dengue. *International Journal of Antimicrobial Agents,* 36**,** S40-S42.

HANSEN, C., HANSEN, E. W., HANSEN, H. R., GAMMELGAARD, B. & STÜRUP, S. 2011. Reduction of Sb (V) in a human macrophage cell line measured by HPLC-ICP-MS. *Biological Trace Element Research,* 144**,** 234-243.

HEIB, T., GROSS, C., MÜLLER, M.-L., STEGNER, D. & PLEINES, I. 2021. Isolation of murine bone marrow by centrifugation or flushing for the analysis of hematopoietic cells – a comparative study. *Platelets,* 32**,** 601-607.

HII, Y. L., ZHU, H., NG, N., NG, L. C. & ROCKLÖV, J. 2012. Forecast of Dengue Incidence Using Temperature and Rainfall. *PLOS Neglected Tropical Diseases,* 6**,** e1908.

HLAKA, L., OZTURK, M., CHIA, J. E., JONES, S. S., PILLAY, S., POSWAYO, S. K. L., MPOTJE, T., NONO, J. K., SIMELANE, S. R. N., PARIHAR, S. P., ROY, S., SUZUKI, H., BROMBACHER, F. & GULER, R. 2021. IL-4i1 Regulation of Immune Protection During Mycobacterium tuberculosis Infection. *J Infect Dis,* 224**,** 2170-2180.

HURDAYAL, R. & BROMBACHER, F. 2017. Interleukin-4 receptor alpha: from innate to adaptive immunity in murine models of cutaneous leishmaniasis. *Frontiers in immunology,* 8**,** 1354.

HURDAYAL, R., H. H. N., MÉLANIE REVAZ-BRETONA, SURAJ P. PARIHARA, JUSTIN KOMGUEP NONOA, MELISSA GOVENDER, AND FRANK BROMBACHER 2017. IL-4–producing B cells regulate T helper cell dichotomy in type 1- and type 2-controlled diseases. *PNAS*.

INBAR, E., HUGHITT, V. K., DILLON, L. A. L., GHOSH, K., EL-SAYED, N. M. & SACKS, D. L. 2017. The Transcriptome of Leishmania major Developmental Stages in Their Natural Sand Fly Vector. *mBio,* 8**,** e00029-17.

IVENS, A. C., PEACOCK, C. S., WORTHEY, E. A., MURPHY, L., AGGARWAL, G., BERRIMAN, M., SISK, E., RAJANDREAM, M.-A., ADLEM, E., AERT, R., ANUPAMA, A., APOSTOLOU, Z., ATTIPOE, P., BASON, N., BAUSER, C., BECK, A., BEVERLEY, S. M., BIANCHETTIN, G., BORZYM, K., BOTHE, G., BRUSCHI, C. V., COLLINS, M., CADAG, E., CIARLONI, L., CLAYTON, C., COULSON, R. M. R., CRONIN, A., CRUZ, A. K., DAVIES, R. M., DE GAUDENZI, J., DOBSON, D. E., DUESTERHOEFT, A., FAZELINA, G., FOSKER, N., FRASCH, A. C., FRASER, A., FUCHS, M., GABEL, C., GOBLE, A., GOFFEAU, A., HARRIS, D., HERTZ-FOWLER, C., HILBERT, H., HORN, D., HUANG, Y., KLAGES, S., KNIGHTS, A., KUBE, M., LARKE, N., LITVIN, L., LORD, A., LOUIE, T., MARRA, M., MASUY, D., MATTHEWS, K., MICHAELI, S., MOTTRAM, J. C., MÜLLER-AUER, S., MUNDEN, H., NELSON, S., NORBERTCZAK, H., OLIVER, K., O'NEIL, S., PENTONY, M., POHL, T. M., PRICE, C., PURNELLE, B., QUAIL, M. A., RABBINOWITSCH, E., REINHARDT, R., RIEGER, M., RINTA, J., ROBBEN, J., ROBERTSON, L., RUIZ, J. C., RUTTER, S., SAUNDERS, D., SCHÄFER, M., SCHEIN, J., SCHWARTZ, D. C., SEEGER, K., SEYLER, A., SHARP, S., SHIN, H., SIVAM, D., SQUARES, R., SQUARES, S., TOSATO, V., VOGT, C., VOLCKAERT, G., WAMBUTT, R., WARREN, T., WEDLER, H., WOODWARD, J., ZHOU, S., ZIMMERMANN, W., SMITH, D. F., BLACKWELL, J. M., STUART, K. D., BARRELL, B., et al. 2005.

The Genome of the Kinetoplastid Parasite, Leishmania major. *Science,* 309**,** 436-442.

JANTSCH, J., SCHATZ, V., FRIEDRICH, D., SCHRÖDER, A., KOPP, C., SIEGERT, I., MARONNA, A., WENDELBORN, D., LINZ, P. & BINGER, K. J. 2015. Cutaneous Na+ storage strengthens the antimicrobial barrier function of the skin and boosts macrophage-driven host defense. *Cell metabolism,* 21**,** 493-501.

JONES, K. E., PATEL, N. G., LEVY, M. A., STOREYGARD, A., BALK, D., GITTLEMAN, J. L. & DASZAK, P. 2008. Global trends in emerging infectious diseases. *Nature,* 451**,** 990-993.

KASAI, S., SHIKU, H., TORISAWA, Y. S., NODA, H., YOSHITAKE, J., SHIRAISHI, T., YASUKAWA, T., WATANABE, T., MATSUE, T. & YOSHIMURA, T. 2005. Real-time monitoring of reactive oxygen species production during differentiation of human monocytic cell lines (THP-1). *Analytica Chimica Acta,* 549**,** 14-19.

KAUFMANN, S. H. E., DORHOI, A., HOTCHKISS, R. S. & BARTENSCHLAGER, R. 2018. Host-directed therapies for bacterial and viral infections. *Nature Reviews Drug Discovery,* 17**,** 35-56.

KAYE, P. & SCOTT, P. 2011. Leishmaniasis: complexity at the host-pathogen interface. *Nature Reviews Microbiology,* 9**,** 604+.

KOPF, M., BROMBACHER, F., KÖHLER, G., KIENZLE, G., WIDMANN, K.-H., LEFRANG, K., HUMBORG, C., LEDERMANN, B. & SOLBACH, W. 1996. IL-4-deficient Balb/c mice resist infection with Leishmania major. *The Journal of experimental medicine,* 184**,** 1127-1136.

LUND, M. E., TO, J., O'BRIEN, B. A. & DONNELLY, S. 2016. The choice of phorbol 12-myristate 13-acetate differentiation protocol influences the response of THP-1 macrophages to a pro-inflammatory stimulus. *Journal of Immunological Methods,* 430**,** 64-70.

LUTZ, M. B., KUKUTSCH, N., OGILVIE, A. L., RÖSSNER, S., KOCH, F., ROMANI, N. & SCHULER, G. 1999. An advanced culture method for generating large quantities of highly pure dendritic cells from mouse bone marrow. *J Immunol Methods,* 223**,** 77-92.

MARQUET, J., LASOUDRIS, F., COUSIN, C., PUIFFE, M.-L., MARTIN-GARCIA, N., BAUD, V., CHEREAU, F., FARCET, J.-P., MOLINIER-FRENKEL, V. & CASTELLANO, F. 2010. Dichotomy between factors inducing the immunosuppressive enzyme IL-4-induced gene 1 (IL4I1) in B lymphocytes and mononuclear phagocytes. *European journal of immunology,* 40**,** 2557-2568.

MERA-RAMÍREZ, A., CASTILLO, A., OROBIO, Y., GÓMEZ, M. A. & GALLEGO-MARIN, C. 2017. Screening of TNFα, IL-10 and TLR4 single nucleotide polymorphisms in individuals with asymptomatic and chronic cutaneous leishmaniasis in Colombia: a pilot study. *BMC Infectious Diseases,* 17**,** 177.

MESSINA, J. P., BRADY, O. J., PIGOTT, D. M., GOLDING, N., KRAEMER, M. U. G., SCOTT, T. W., WINT, G. R. W., SMITH, D. L. & HAY, S. I. 2015. The many projected futures of dengue. *Nature Reviews Microbiology,* 13**,** 230-239.

MILLS, C. D. 2015. Anatomy of a discovery: m1 and m2 macrophages. *Front Immunol,* 6**,** 212.

MO, R. H., ZARO, J. L., OU, J.-H. J. & SHEN, W.-C. 2012. Effects of Lipofectamine 2000/siRNA complexes on autophagy in hepatoma cells. *Molecular biotechnology,* 51**,** 1-8.

MODOLELL, M., CORRALIZA, I. M., LINK, F., SOLER, G. & EICHMANN, K. 1995. Reciprocal regulation of the nitric oxide synthase/arginase balance in mouse bone marrow-derived macrophages by TH 1 and TH 2 cytokines. *European journal of immunology,* 25**,** 1101-1104.

MOHRS, M., HOLSCHER, C. & BROMBACHER, F. 2000. Interleukin-4 Receptor Alpha-Deficient BALB/c Mice Show an Unimpaired T Helper 2 Polarization in Response to Leishmania major Infection. *Infection and Immunity,* 68**,** 1773.

MOHRS, M., LEDERMANN, B., KÖHLER, G., DORFMÜLLER, A., GESSNER, A. & BROMBACHER, F. 1999. Differences Between IL-4- and IL-4 Receptor α-Deficient Mice in Chronic Leishmaniasis Reveal a Protective Role for IL-13 Receptor Signaling. *The Journal of Immunology,* 162**,** 7302.

MOJTAHEDI, Z., CLOS, J. & KAMALI-SARVESTANI, E. 2008. Leishmania major: Identification of developmentally regulated proteins in procyclic and metacyclic promastigotes. *Experimental Parasitology,* 119**,** 422-429.

MOLINIER-FRENKEL, V., PRÉVOST-BLONDEL, A. & CASTELLANO, F. 2019. The IL4I1 enzyme: a new player in the immunosuppressive tumor microenvironment. *Cells,* 8**,** 757.

MORENS, D. M., FOLKERS, G. K. & FAUCI, A. S. 2004. The challenge of emerging and re-emerging infectious diseases. *Nature,* 430**,** 242-249.

MUKHOPADHYAY, J., BRAIG, H. R., ROWTON, E. D. & GHOSH, K. 2012. Naturally occurring culturable aerobic gut flora of adult Phlebotomus papatasi, vector of Leishmania major in the Old World. *PloS one,* 7**,** e35748-e35748.

MUNITA, J. M. & ARIAS, C. A. 2016. Mechanisms of Antibiotic Resistance. *Microbiol Spectr,* 4.

MURRAY, H. W. 2001. Clinical and experimental advances in treatment of visceral leishmaniasis. *Antimicrobial agents and chemotherapy,* 45**,** 2185-2197.

MURRAY, H. W. & HARIPRASHAD, J. 1995. Interleukin 12 is effective treatment for an established systemic intracellular infection: experimental visceral leishmaniasis. *Journal of Experimental Medicine,* 181**,** 387-391.

MURRAY, H. W., MIRALLES, G. D., STOECKLE, M. Y. & MCDERMOTT, D. F. 1993. Role and effect of IL-2 in experimental visceral leishmaniasis. *J Immunol,* 151**,** 929-38.

NELMS, K., KEEGAN, A. D., ZAMORANO, J., RYAN, J. J. & PAUL, W. E. 1999. The IL-4 receptor: signaling mechanisms and biologic functions. *Annu Rev Immunol,* 17**,** 701-38.

NOBEN-TRAUTH, N., KROPF, P. & MULLER, I. 1996. Susceptibility to Leishmania major infection in interleukin-4-deficient mice. *Science,* 271**,** 987.

OSERO, B. O. O., ARULEBA, R. T., BROMBACHER, F. & HURDAYAL, R. 2020. Unravelling the unsolved paradoxes of cytokine families in host resistance and susceptibility to Leishmania infection. *Cytokine: X,* 2**,** 100043.

PALMA, D., MERCURIALI, L., FIGUEROLA, J., MONTALVO, T., BUENO-MARÍ, R., MILLET, J.-P., SIMÓN, P., MASDEU, E. & RIUS, C. 2021. Trends in the Epidemiology of Leishmaniasis in the City of Barcelona (1996–2019). *Frontiers in Veterinary Science,* 8.

PARIHAR, S. P., HARTLEY, M.-A., HURDAYAL, R., GULER, R. & BROMBACHER, F. 2016. Topical simvastatin as host-directed therapy against severity of cutaneous leishmaniasis in mice. *Scientific reports,* 6**,** 33458.

PAVLI, A. & MALTEZOU, H. C. 2010. Leishmaniasis, an emerging infection in travelers. *International Journal of Infectious Diseases,* 14**,** e1032-e1039.

PETERSEN, E., PETROSILLO, N., KOOPMANS, M., BEECHING, N., DI CARO, A., GKRANIA-KLOTSAS, E., KANTELE, A., KOHLMANN, R., KOOPMANS, M., LIM, P. L., MARKOTIC, A., LÓPEZ-VÉLEZ, R., POIREL, L., ROSSEN, J. W. A., STIENSTRA, Y. & STORGAARD, M. 2018. Emerging infections—an increasingly important topic: review by the Emerging Infections Task Force. *Clinical Microbiology and Infection,* 24**,** 369-375.

PUIFFE, M. L., LACHAISE, I., MOLINIER-FRENKEL, V. & CASTELLANO, F. 2013. Antibacterial properties of the mammalian L-amino acid oxidase IL4I1. *PLoS One,* 8**,** e54589.

REALES-CALDERÓN, J. A., VAZ, C., MONTEOLIVA, L., MOLERO, G. & GIL, C. 2017. Candida albicans Modifies the Protein Composition and Size Distribution of THP-1 Macrophage-Derived Extracellular Vesicles. *J Proteome Res,* 16**,** 87-105.

REITER, P., LATHROP, S., BUNNING, M., BIGGERSTAFF, B., SINGER, D., TIWARI, T., BABER, L., AMADOR, M., THIRION, J., HAYES, J., SECA, C., MENDEZ, J., RAMIREZ, B., ROBINSON, J., RAWLINGS, J., VORNDAM, V., WATERMAN, S., GUBLER, D., CLARK, G. & HAYES, E. 2003. Texas lifestyle limits transmission of dengue virus. *Emerging infectious diseases,* 9**,** 86-89.

RIBEIRO, C. V., ROCHA, B. F. B., OLIVEIRA, E., TEIXEIRA-CARVALHO, A., MARTINS-FILHO, O. A., MURTA, S. M. F. & PERUHYPE-MAGALHÃES, V. 2020. Leishmania infantum induces high phagocytic capacity and intracellular nitric oxide production by human proinflammatory monocyte. *Memórias do Instituto Oswaldo Cruz,* 115.

RØTTINGEN, J.-A., GOUGLAS, D., FEINBERG, M., PLOTKIN, S., RAGHAVAN, K. V., WITTY, A., DRAGHIA-AKLI, R., STOFFELS, P. & PIOT, P. 2017. New Vaccines against Epidemic Infectious Diseases. *New England Journal of Medicine,* 376**,** 610-613.

ROY, S., SCHMEIER, S., ARNER, E., ALAM, T., PARIHAR, S. P., OZTURK, M., TAMGUE, O., KAWAJI, H., DE HOON, MICHIEL J. L., ITOH, M., LASSMANN, T., CARNINCI, P., HAYASHIZAKI, Y., FORREST, ALISTAIR R. R., BAJIC, V. B., GULER, R., CONSORTIUM, F., BROMBACHER, F. & SUZUKI, H. 2015. Redefining the transcriptional regulatory dynamics of classically and alternatively activated macrophages by deepCAGE transcriptomics. *Nucleic Acids Research,* 43**,** 6969-6982.

SACKS, D. & KAMHAWI, S. 2001. Molecular Aspects of Parasite-Vector and Vector-Host Interactions in Leishmaniasis. *Annual Review of Microbiology,* 55**,** 453-483.

SACKS, D. & NOBEN-TRAUTH, N. 2002. The immunology of susceptibility and resistance to Leishmania major in mice. *Nat Rev Immunol,* 2**,** 845-58.

SCHMITTGEN, T. D. & LIVAK, K. J. 2008. Analyzing real-time PCR data by the comparative C(T) method. *Nat Protoc,* 3**,** 1101-8.

SEDDIGH, P., BRACHT, T., MOLINIER-FRENKEL, V., CASTELLANO, F., KNIEMEYER, O., SCHUSTER, M., WESKI, J., HASENBERG, A., KRAUS, A., POSCHET, G., HAGER, T., THEEGARTEN, D., OPITZ, C. A., BRAKHAGE, A. A., SITEK, B., HASENBERG, M. & GUNZER, M. 2017. Quantitative Analysis of Proteome Modulations in Alveolar Epithelial Type II Cells in Response to Pulmonary Aspergillus fumigatus Infection. *Molecular & cellular proteomics : MCP,* 16**,** 2184-2198.

SEREZANI, C. H., PERRELA, J. H., RUSSO, M., PETERS-GOLDEN, M. & JANCAR, S. 2006. Leukotrienes Are Essential for the Control of Leishmania amazonensis Infection and Contribute to Strain Variation in Susceptibility. *The Journal of Immunology,* 177**,** 3201.

SOUZA, M. D. A., RAMOS-SANCHEZ, E. M., MUXEL, S. M., LAGOS, D., REIS, L. C., PEREIRA, V. R. A., BRITO, M. E. F., ZAMPIERI, R. A., KAYE, P. M., FLOETER-WINTER, L. M. & GOTO, H. 2021. miR-548d-3p Alters Parasite Growth and Inflammation in Leishmania (Viannia) braziliensis Infection. *Frontiers in Cellular and Infection Microbiology,* 11.

STEVERDING, D. 2017. The history of leishmaniasis. *Parasites & Vectors,* 10**,** 82.

SUNDAR, S. & MURRAY, H. W. 1995. Effect of treatment with interferon-gamma alone in visceral leishmaniasis. *J Infect Dis,* 172**,** 1627-9.

TSUCHIYA, S., YAMABE, M., YAMAGUCHI, Y., KOBAYASHI, Y., KONNO, T. & TADA, K. 1980. Establishment and characterization of a human acute monocytic leukemia cell line (THP-1). *Int J Cancer,* 26**,** 171-6.

ULUSAN, Ö., MERT, U., SADIQOVA, A., ÖZTÜRK, S. & CANER, A. 2020. Identification of gene expression profiles in Leishmania major infection by integrated bioinformatics analyses. *Acta Tropica,* 208**,** 105517.

YUE, Y., HUANG, W., LIANG, J., GUO, J., JI, J., YAO, Y., ZHENG, M., CAI, Z., LU, L. & WANG, J. 2015. IL4I1 Is a Novel Regulator of M2 Macrophage Polarization That Can Inhibit T Cell Activation via L-Tryptophan and Arginine Depletion and IL-10 Production. *PLoS One,* 10**,** e0142979.

ZELLWEGER, R. M., CANO, J., MANGEAS, M., TAGLIONI, F., MERCIER, A., DESPINOY, M., MENKÈS, C. E., DUPONT-ROUZEYROL, M., NIKOLAY, B. & TEURLAI, M. 2017. Socioeconomic and environmental determinants of dengue transmission in an urban setting: An ecological study in Nouméa, New Caledonia. *PLOS Neglected Tropical Diseases,* 11**,** e0005471.

ZUMLA, A., RAO, M., WALLIS, R. S., KAUFMANN, S. H., RUSTOMJEE, R., MWABA, P., VILAPLANA, C., YEBOAH-MANU, D., CHAKAYA, J., IPPOLITO, G., AZHAR, E., HOELSCHER, M. & MAEURER, M. 2016. Host-directed therapies for infectious diseases: current status, recent progress, and future prospects. *Lancet Infect Dis,* 16**,** e47-63.

6. Appendix

Table S1: List of murine flow cytometry antibodies used

Antibodies	Murine
CD11b	Biocom Africa, catalogue number 117310, 100 μg
F4/80	Biocom Africa, catalogue number 123114, 100 μg

Table S2: List of human flow cytometry antibodies used

Antibodies	Human
CD16	Clone 3G8, catalogue number 302010, 100 μg
CD14	Clone M5E2, catalogue number 301836, 100 μg
CD64	Clone 10.1, catalogue number 305007, 100 μg

Table S3: List of ELISA antibodies used

Antibodies	Murine	Human
IL-10	Standard: WhiteSci, clone number 417-ML-005, [100 ng/ml];	
	Primary Abs: WhiteSci, clone number MAB417-500, [1 μg/ml];	Primary: PharMingen, clone number 20701D [0.5 mg/ml]
	Secondary Abs: Biocom Biotech, clone number 504906, [0.5 μg/ml]	Secondary: PharMingen, clone number 18562D [0.5 mg/ml]
IL-12	Standard: Biocom, clone number C18.2 [50 μg/ml]	
	Primary: WhiteSci, catalogue number 419-ML-010 [10 μg/ml]	Primary: PharMingen, clone number 23271D [0.5 mg/ml]
	Secondary: BD Bioscience, clone number 554476 [0.5 mg/ml]	Secondary: PharMingen, clone number 20512D [0.5 mg/ml]